A

Dissertation Report

On

Effect of functionalization on the thermal conductivity of CNT/polymer nanocomposites using reverse non-equilibrium molecular dynamics simulations

Submitted in Partial Fulfillment of the Requirements for the Award of Degree of

Master of Technology

In

Design Engineering

By

Ankit Chauhan

2015PDE5202

Under the supervision of

Dr. Dinesh Kumar
Assistant Professor
Department of Mechanical Engineering
MNIT, Jaipur, India

DEPARTMENT OF MECHANICAL ENGINEERING
MALAVIYA NATIONAL INSTITUTE OF TECHNOLOGY, JAIPUR
JUNE 2017

A

Dissertation Report

On

Effect of functionalization on the thermal conductivity of CNT/polymer nanocomposites using reverse non-equilibrium molecular dynamics simulations

Submitted in Partial Fulfillment of the Requirements for the Award of Degree of

Master of Technology

In

Design Engineering

By

Ankit Chauhan

2015PDE5202

Under the supervision of

Dr. Dinesh Kumar
Assistant Professor
Department of Mechanical Engineering
MNIT, Jaipur, India

DEPARTMENT OF MECHANICAL ENGINEERING
MALAVIYA NATIONAL INSTITUTE OF TECHNOLOGY, JAIPUR
JUNE 2017

DEPARTMENT OF MECHANICAL ENGINEERING,
MALAVIYA NATIONAL INSTITUTE OF TECHNOLOGY,
JAIPUR-302017 (RAJASTHAN).

CERTIFICATE

This is certified that the dissertation report entitled **"Effect of functionalization on the therml conductivity of CNT/polymer nanocomposites using reverse non-equilibrium molecular dynamics simulations"** prepared and submitted by **Ankit Chauhan** (ID-2015PDE5202), in the partial fulfillment of the award of the Degree **Master of Technology** in **Design Engineering** of Malaviya National Institute of Technology Jaipur, is a record of bonafide research work carried out by him under my supervision and is hereby approved for submission. The contents of this dissertation work, in full or in parts, have not been submitted to any other Institute or University for the award of any degree or diploma.

Date:

Place:

Dr. DINESH KUMAR
Assistant Professor
Department of Mechanical Engineering
MNIT, Jaipur, India

DEPARTMENT OF MECHANICAL ENGINEERING,
MALAVIYA NATIONAL INSTITUTE OF TECHNOLOGY,
JAIPUR-302017 (RAJASTHAN).

DECLARATION

I, **Ankit Chauhan** (ID-2015PDE5202) hereby declare that the dissertation entitled **"Effect of functionalization on the thermal conductivity of CNT/polymer nanocomposites using non-equilibrium molecular dynamics"** being submitted by me in partial fulfillment of the degree of **M. Tech (Design Engineering)** is a research work carried out by me under the supervision of **Dr. Dinesh Kumar,** and the contents of this dissertation work, in full or in parts, have not been submitted to any other Institute or University for the award of any degree or diploma. I also certify that no part of this dissertation work has been copied or borrowed from anyone else. In case any type of plagiarism is found out, I will be solely and completely responsible for it.

Date: **Ankit Chauhan**

M.Tech. (Design Engg.)

Place: **2015PDE5202**

ACKNOWLEDGEMENT

I feel immense pleasure in conveying my heartiest thanks and profound gratitude to my supervisor **Dr. Dinesh Kumar,** who provided me with his generous guidance, valuable help and endless encouragement by taking personal interest and attention. No words can fully convey my feelings of respect and regard for him. I would like to thank **Mr. Ashish Kumar Srivastava** and **Mr. Akhileshwar Singh,** Ph.D scholars and members of the research group, for their support and help in this piece of work.

I also express my deepest gratitude to my **parents** for their blessings and affection, without which I would have not be able to endure hard time and carry on. Lastly, but not least I thank one and all who have helped me directly or indirectly in completion of the dissertation.

Date: **Ankit Chauhan**

M.Tech. (Design Engg.)

Place: **2015PDE5202**

ABSTRACT

The aim of present study is to investigate the effect of functionalization on the thermal conductivity of CNT/polymer nanocomposite. Reverse non-equilibrium molecular dynamics (RNEMD) simulations is employed to predict the thermal conductivity of the system. Molecular dynamics (MD) simulations are performed using the Large-scale Atomic/Molecular Massively Parallel Simulator (LAMMPS). The thermal conductivity of single-walled carbon nanotube (SWCNT) is evaluated and verified with the available results in literature. Thereafter, parametric studies are conducted to investigate the effects of interatomic potentials (namely Tersoff, AIREBO, REBO and Optimized Tersoff), and temperature on the thermal conductivity of SWCNT. Subsquently, the simulations are also carried out to estimate the thermal conductivity of polyethylene matrix using polymer consistent force field (PCFF). Further, parametric studies are conducted to find the effect of the chain length and temperature on thermal conductivity of polyethylene matrix. It is established that, the thermal conductivity of polyethelene matrix increases with the increase in chain length of polyethylene as well as temperature. In the last section of this thesis, a SWCNT/polyethylene nanocomposites is modelled and the effect of functionalization on the thermal conductivity of nanocomposite is studied. Carboxylic (-COOH) group is utilized for functionalization of SWCNTs. It is reported that, with the increase in functionalization, the coupling between the SWCNT and the polyethylene matrix increases which leads to the increase in the thermal conductivity of nanocomposite material.

TABLE OF CONTENT

LIST OF FIGURES

LIST OF TABLES

LIST OF ABBREVIATIONS

CNT	Carbon nanotube
SWCNT	Single-wall carbon nanotube
MWCNT	Multi-walled carbon nanotube
DNA	Deoxyribonucleic acid
MFP	Mean-free-path
EMD	Equilibrium molecular dynamics
NEMD	Non-equilibrium molecular dynamics
HNEMD	Homogeneous non-equilibrium molecular dynamics
MD	Molecular dynamics
REBO	Reactive empirical bond order
LJ	Lennard-Jones
AIREBO	Adaptive intermolecular reactive empirical bond order
LDPE	Low density polyethylene
HDPE	High density polyethylene
PP	Polypropylene
PS	Polystyrene
PMMA	Polymethylmethacrylate
COOH	Carboxylic acid
RNEMD	Reverse non-equilibrium molecular dynamics
PCFF	Polymer consistent force field
CFF	Consistent force field
CVFF	Consistent valence force field
LAMMPS	Large-scale atomic/molecular massively parallel simulator

Chapter 1

1 Introduction

1.1 About CNT

A CNT is a cylindrical tube made of carbon atoms and exists either as a single-walled structure, known as single wall carbon nanotube (SWCNT) or as multilayered structure, known as a multi-walled carbon nanotube (MWCNT) [1]. Multi-walled carbon nanotubes were first discovered by Iijima [2] in 1991, and single-walled carbon nanotubes by Iijima and Ichihashi [3] and Bethune et al. [4] in 1993. There is a wide range of applications in which carbon nanotubes (CNTs) are used such as molecular transporters, sensors, surgical aids etc. CNT is used as a nano channel as its center core is hollow. [1]. CNTs have received much attention due to its unique mechanical [5–8], thermal [9–11] and electrical properties [6]. Experimental results reported in literatures [9–14] show the high thermal conductivity of the CNT because of atoms are held together in the CNT by strong sp^2 bonds [15,16]. CNT based materials are using for future space vehicles. CNTs have Young's modulus over 1 Tera Pascal [5–8]. CNTs can be either metallic or semiconductor depending on their chirality. Armchair (n,n) SWNTs have electrical properties that are metallic. Zig-zag(n,0) and chiral(n,m) SWNTs are metallic if n-m/3=0; otherwise, they are semiconducting. The thermal conductivity of CNTs depends on atomic arrangement, the diameter and length of the tubes, the number of structural defects and the morphology, as well as on the presence of impurities [17–21]. Recently, nanotechnology has gained much attention in research to develop materials. It is one of the fastest growing areas in material science [22]. The improvement in the thermal conductivity of polymers has been observed with different nanoparticles [23]. CNTs is one of them and have been intensively studied as an ultimate filler in polymer nanocomposites for thermal management because of their high flexibility [24,25]. However, it has been observed that addition of CNTs as filler material in to polymer matrix, the thermal conductivity of the resulting nanocomposites is decreased. The reason behind is the presence of thermal resistance of interface between the CNT and the polymer matrix. The interfacial thermal resistance can be alleviated by functionalization [26]. In this study, the objective is to investigate the effect of

carboxylic acid (-COOH) functional group on the thermal conductivity of SWCNT/polyethylene nanocomposites.

1.2 Conduction Phenomena in CNT and Polymers

In the SWCNTs, thermal transport phenomenon is generally categorized in three different regimes. If the tube length is smaller than effective phonon mean free path (MFP), the thermal transport is ballistic wherein the thermal resistance due to phonon boundary scattering dominates over the phonon-phonon scattering. The diffusive regime is defined when the thermal conductivity becomes independent of increasing the length which occurs when the tube length is greater than the diffusive transition length. Here the thermal resistance is caused by phonon-phonon scattering. When both phonon boundary scattering and phonon-phonon scattering co-exist, the regime is called ballistic-diffusive transition. There is a gradual transition from the ballistic regime to the diffusive regime in between the MFP and the diffusive transition length [20,27–29].

In the most of the polymers, phonons, that are quantized modes of vibration occurring in a rigid crystal lattice in the absence of free electrons movement, are the primary mechanism behind the thermal transport. While for amorphous polymers, the thermal conductivity is very low as the phonon MFP is very small [22, 30, 31].

Chapter 2

2 Literature Review

2.1 Thermal Conductivity of Carbon Nanotubes

Many studies have reported the thermal conductivity of the CNTs calculated using various methods, viz. equilibrium molecular dynamics (EMD) [17, 32], non-equilibrium molecular dynamics (NEMD) [16, 18, 20, 27, 29, 33–35] and homogeneous non-equilibrium molecular dynamics (HNEMD) [15]. Table 1 summarize the works done on calculation of thermal conductivity of CNTs. All the results shown in the Table 1 are for (10,10) SWCNT at 300 K using the MD simulations. Variations in the results can be seen in Table 1 even for the same length of CNT and potential used. On the other hand, for the experimental results shown in Table 2, chirality is unknown while thermal conductivity values are predicted at 300 K. Further, Berber and Tománek [15] reported an unusually high thermal conductivity value of 37000 W/m/k at 100 K and showed a decreasing trend of thermal conductivity with increase in temperature (6600W/m/k at 300 K). On the contrary, Osman and Srivastava [33] reported the increasing trend of thermal conductivity value from 100 K to 400 K followed by a drop at 500K. They established the thermal conductivity value of 1700 W/m/k at room temperature 300 K. Che et al. [17] found that the thermal conductivity value to 2980 W/m/k at 300 K and showed the convergence of thermal conductivity at 10 nm. Cao and Qu [20] found the thermal conductivity value 1580 W/m/k for the length of 4800 nm at 300 K. Padgett and Brenner [16] found the value 36-348 W/m/k of thermal conductivity for length in the range 10-310 nm and showed the convergence of thermal conductivity from 150 nm. Thomas et al. [29] found the value in between 300-365 W/m/k for the length taken in the range 200 – 1000 nm and didn't show the convergence for the same potential as used in [16]. Both Maruyama, Engineering, and Taylor [34] and Moreland [18] used the same potential and found the value of thermal conductivity 275 W/m/k for the length 6 nm of CNT, while Taylor [34] found the value of thermal conductivity 215 W/m/k for the length 50 nm. Lukes and Zhong [32] found the value 20-160 W/m/k for the length range 5-40 nm and Salaway and Zhigilei [27] found the value of

155-264 W/m/k for the length 47 nm to 630 nm. Therefore, it can be noted that there is a significant difference between the results even for the same potential. Many researchers have tried to find out the discrepancies in the results published in the literature. As cross-section area plays an important role to find the thermal conductivity, so that could be one of the reasons. Che et al. [17] had chosen a ring of 1 A^0 thickness for CNT, while the others [16, 19, 20, 27, 29, 33–36] considered a ring thickness of 3.4 A^0. Salaway and Zhigilei [27] suggested that uncertainty in the interpretation of the results can be caused by the common practice of neglecting the length of the heat bath regions when defining the CNT length. In addition, Lukes and Zhong [32] observed that HNEMD method was found to give a factor of 3-12 times higher than the EMD method for the same length of CNT. However, Salaway and Zhigilei [27] suggested not to compare the results for different interatomic potentials based on the observation that fourfold difference in the values of thermal conductivity is possible for the identical CNTs and computational setups, but predicted for only one length of CNT (i.e., 205 nm).

Table 1 Thermal conductivity for (10,10) SWCNTs reported in the literature at 300 K.

Reference	K (W/m/k)	Length (nm)	Potential	Method	Boundary Conditions
Savas Berber and David Tománek [15]	6600	2.5	Tersoff 1988b	HNEMD	Periodic
Che et al. [17]	2980	40	Brenner 1990	EMD	Periodic
Osman and Srivastava [33]	1700	30	Brenner 1990	NEMD	Periodic
Maruyama, Engineering, and Taylor[34]	275-390	6-404	Brenner 1990	NEMD	Non-periodic
Moreland [18]	215-831	50-1000	Brenner 1990	NEMD	Periodic
Padgett and Brenner [16]	36-348	10-310	REBO	NEMD	Periodic
Thomas et al. [29]	300-365	200-1000	REBO	NEMD	Non-periodic
Lukes and Zhong [32]	20 - 160	5-40 nm	REBO + LJ	EMD	Periodic and non-periodic
Salaway and Zhigilei [27]	155-264	47-630	AIREBO	NEMD	Non-periodic
Cao and Qu [20]	1580	4800	Optimized Tersoff	NEMD	Periodic

Table 2 Thermal conductivity of CNTs observed experimental at 300 K.

Reference	K (W/m/k)	Length (nm)	Diameter (nm)	Experiment	Type
Pop et al. [9]	3500	2600	1.7	Self-heating	SWCNT
Fuji et al. [13]	2800	3700	9.8	T-type sensor	MWCNT
Yu et al. [10]	2000-10000	2600	3-1	Heater sensor	SWCNT
Kim et al. [11]	> 3000	2500	14	Heater sensor	MWCNT
Pettes and Shi [14]	> 600	4310	2.33	Heater sensor	SWCNT

2.2 Thermal Conductivity of Polymers

Polymer materials, both natural and synthetic, due to their unique properties like toughness, viscoelasticity, and ability to form glasses and semi-crystalline structures rather than crystal, make them play an essential role in everyday life. In recent years, with the advancement in nanofluidics and nanotechnology, polymer nanostructures have attracted researchers for their wide potential applications in areas such as mechatronics, fluidic nanodevices, medicine and photonics [37]. Thermal conductive polymeric materials are superior to metals in electronics, colling systems, heat transfers from the chemical resistance point of view [38]. Polymers have many applications but are often limited by their inherent physical properties. Most of the polymers have very low thermal conductivity of the order of 0.1-1 W/m/k at room temperature, which is one of the major roadblocks for polymer-based microelectronics and macroelectronics such as organic displays and organic solar cells, due to their limited heat spreading capability [38, 39]. The thermal conductivity of polymers is an important thermal property. Polymers have low thermal conductivity, which makes them suitable to use as good thermal insulators. However, in other applications which require higher thermal conductivity, such as in electronic packaging and encapsulations, heat exchangers, machinery, satellite devices and in areas where

good heat dissipation, low thermal expansion, and light weight are needed, polymers are reinforced with fillers, organic or inorganic, are becoming more and more common in producing advanced polymer composites for these applications [22, 30].

The primary mechanism behind the thermal transport in most of the polymers is phonons. Table 3 displays the thermal conductivities of some polymers, as tabulated in Ref. [22]. Factors mainly temperature, pressure, the degree of crystallinity, the density of the polymer, crystal structures and orientation of chain segments significantly affect thermal conductivity of polymers [30], but out of these, it is strongly affected by its crystallinity. For instance, for amorphous polymers, such as polystyrene (PS) or polymethylmethacrylate (PMMA), the thermal conductivity has a value near to 0.2 W/m/k, whereas, for highly crystalline polymers such as high-density polyethylene (HDPE) the value is to 0.5 W/m/k [40]. At the same time, thermal conductivity of an amorphous polymer increases with rise in temperature up to the glass transition temperature beyond which it falls [41]. But the study by Kline [42] shows that the thermal conductivity of some polymers (PE, PS, PTFE and epoxy resin) increases with temperature varied from 273 – 373 K, and also found that the thermal conductivity is higher in crystalline than amorphous region.

Table 3 Thermal conductivity of different polymers [22].

Polymer	Thermal Conductivity at 298 K(W/m/K)
Low density polyethylene (LDPE)	0.3
High density polyethylene (HDPE)	0.44
Polypropylene (PP)	0.11
Polystyrene (PS)	0.14
Polymethylmethacrylate (PMMA)	0.21

2.3 Thermal Conductivity of Nanocomposites

Polymer composites have been widely used for its application in industries as structural and cushion materials, electromagnetic and heat shields, sensors, catalyst and conducting plastics. Nanomaterials used as fillers such as CNTs, graphene, fullerenes, dendrimers, inorganic nanoparticles and bio-nanoparticles are used to enhance the mechanical, thermal and electrical conductivity of polymers [24]. Among these various nanofillers, CNTs, made up of concentric graphene cylinders and having sp^2 bond between carbon atoms, have been intensively studied as an ultimate filler in polymer nanocomposites for thermal management because of their high

flexibility, low mass density, large aspect ratio and very high thermal conductivity [24, 25]. Efficient heat removal has become an important issue regarding performance and progress in minimizing of pieces in photonic, optoelectronic, electronic and electromagnetic shielding devices [43]. Recently, development of next generation like integrated circuits, ultrafast high power density communication devices, etc. need the efficient high thermal management for its applications [44]. Thermal conductive polymeric materials are used that are superior to metals in electronic engineering, cooling systems, and heat transfers because its advantages include induced density, increased corrosion, oxidation, chemical resistance, and increased processability [38].

Nanotechnology has gained much attention in research to develop materials. It can be broadly defined as the creation, processing, characterization, and use of materials, devices, and systems with the dimensions in the range 0.1-100 nm, exhibiting novel or significantly enhanced physical, chemical and biological properties, functions due to their nanoscale size. Nanotechnology is one of the fastest growing areas in materials science and engineering [22]. The improvement in the thermal conductivity of polymers has been observed with different nanoparticles. The thermal conductivity of PS and PMMA with 24 wt. % boron nitride nanotubes as filler was observed as 3.61 and 2.50 W/m/k, respectively [23]. The thermal conductivity for HDPE filled with 7 vol. % nanometer size expanded graphite was 1.59 W/m/k, twice that of micro-composites (0.78 W/m/k) at the same volume [38]. Hong and Tai [45] observed ten-fold in the thermal conductivity for 1 wt. % SWCNT/PMMA nanocomposites compared to PMMA alone. Cai and Song [46] reported that 3 wt. % of multiwalled CNTs reinforced within polyurethane increases the thermal conductivity to 210 %. Kim et al. [25] demonstrated an enhancement of thermal conductivity from 250 to 393 W/m/k for 7 wt. % of CNTs filled within phenolic resin. Gardea and Lagoudas [47] reported the increase of 125 % or higher in thermal conductivity for some SWCNT/epoxy nanocomposites with CNT reinforement of only 1.0 wt. %. On the contrary, Moisala et al. [47] reported a decrease in thermal conductivity for SWCNT/ epoxy composites with increase in wt. fraction, compared to neat epoxy. Experiments and molecular modeling studies have revealed that the resistance to the heat flow caused by CNT-polymer interface is the reason for the low thermal conductivity. The interface thermal resistance, also called as the Kapitza resistance, is important due to its small size and high surface-to-volume ratio in nanocomposites, filled with nanostructured fillers [48]. The reason behind is the weak coupling of phonons between unfuntionalized CNT and the polymeric matrix materials [47]. This problem can be alleviated

by chemical modification to the CNTs. It has been found that functionalization leads to the larger thermal conductivity of CNT nanocomposites within 100-1000 aspect ratio range, while for larger aspect ratios, unfuntionalized CNTs composites are better thermal conductors [26]. It was also observed that the enhancement of thermal conductivity to 16 times of polymer for aligned composites by increasing the degree of dispersion, the volume fraction of CNT and the length of CNT [49]. And functionalization of CNTs is found to be effective in enhancing the dispersion [24].

2.4 Thermal Conductivity of Functionalized Nanocomposites

The functionalization of CNTs can be done by covalent and noncovalent methods of the use of different substances, such as chemical groups [50], metals [51], polymers [52] and surfactants [53]. Covalent bonds help to form the bridge and allow the transfer of phonons between the CNTs and the polymer matrix [22]. Functionalization leads to change the sp^2 bonds to sp^3 bonds, which results in the increase of sp^3 bonded carbon atoms in the nanotubes. This conversion creates scattering centers for acoustic phonon propagating along the CNT, reduces the MFP of the phonons, which ultimately reduces the thermal conductivity of the CNTs [16]. Although, the impact of disrupted conjugation have an intense impact on thermal conductivity, while it is found to be limited for mechanical properties [22]. It was found that significant drop in thermal conductivity with 1 % of carbon atoms, while further increase in the degree of functionalization did not result in lowering the thermal conductivity [16, 26].. The non-covalent functionalization includes surfactant modification of CNT, polymer wrapping or absorption between the CNT and the functional group, and the main advantage of non-covalent functionalization is that properties remain unchanged as the structure in not damaged. But, the main disadvantage is the high interfacial thermal resistance, which may be due to weak forces between the CNT and the wrapping molecules [22].

Clancy et al. [39] used covalent chemical functionalization and modelled the grafting linear hydrocarbon chains to the surface of an SWCNT and reported that the decrease in the interfacial thermal resistance leads to significant increase in thermal conductivity of nanocomposites comprised of SWCNT and the polyethylene vinyl acetate polymer matrix. Shenogin et al. [26] reported decrease in the interfacial resistance by more than three times when CNTs were functionalized with octane molecule. Gulotty et al. [54] observed an enhancement of 25 % in the thermal conductivity of nanocomposite by adding the SWCNTs in to the epoxy, but thermal conductivity dropped almost to the neat epoxy value when SWCNT was functionalized

at 3 wt. %. Hong and Tai [45] showed an enhancement in thermal conductivity of SWCNT/PMMA nanocomposite from 0.60 W/m/k for purified SWCNT to 2.43 W/m/k for COOH functionalized SWCNT.

2.5 Associated Critical Issues

There are two main critical issues, in general, of practical concerns associated with the use of CNTs in polymer nanocomposites which are also applicable when CNTs are used as thermally conductive fillers. These are: (1) aggalomaration- means that CNTs form bundles when mixed in polymeric matrix as CNTs have large surface areas and possess large van der Waals forces [48, 53, 55], and (2) interface effects- the interfacial thermal resistance between the CNT and the polymeric matrix which leads to a reduction of thermal transport properties [56].

2.6 Objective

The development and quality of CNT-polymer nanocomposites, in terms of its mechanical, thermal, electrical properties, will depend on number of factors such as length of CNTs, diameter, aspect ratio, loading of CNTs, the interaction between the CNT and the matrix, alignment, and dispersion. However, there are no systematic studies investigating the effects of nanofiller purity, aspect ratio, type of functional group and degree of functionalization on the overall properties of nanocomposites. Keeping in consideration the literature review and one of the critical issues-interfacial effects, the objective of present work is to investigate the effect of functionalization, at the interface between the CNT and the polymeric matrix, on the thermal conductivity of CNT/polymer nanocomposites.

2.7 Present Study

The aim of present thesis work is to study the effect of functionalization on the thermal conductivity of SWCNT/polyethylene nanocomposites using polymer consistent force field (PCFF) [57]. Reverse non-equilibrium molecular dynamics (RNEMD) simulation is used to calculate the thermal conductivity of the nanocomposites. Initially, the thermal conductivity of (10,10) armchair pristine SWCNT is calculated using different interatomic potentials, namely Tersoff [58], AIREBO [59], REBO [60] and Optimized Tersoff [61] at 300 K temperature. Thereafter, the effect of temperature on the thermal conductivities of (10,10), (24,0) and (14,14) SWCNTs are studied. MD simulations were performed to find the effect of chain length

(obtained by different numbers of monomers, i.e., 10, 50, 100, 150 and 200) of polyethylene polymer on the its thermal conductivity at 300 K. Further, to study the effect of temperature on the thermal conductivity of polyethylene polymer made of different chain lengths, simulation were run at different temperature taken in the range 275 - 350 K. Finally, effect of functionalization on the thermal conductivity of SWCNT/polyethylene nanocomposites was investigated by functionalizing different percentages (i.e., 1%, 3%, 5%) of carbon atoms of SWCNT with -COOH functional group and subsequently, reinforcing the same in to polyethylene polymer matrix, made by chain length of 200 monomers.

Chapter 3

3 Molecular Dynamics

3.1 Introduction

Classical MD simulations are based on Newton's second law of equation for atoms interacting with each other through an interatomic potential. By integrating Newton's second law of motion using different integration algorithms, the atomic trajectories of atoms in space and time using the calculated acceleration values of the atoms is determined [1]. It is given by

$$F_i = m_i a_i,$$

where, F_i is the force on atom i and can be obtained from the negative derivative of the potential energy with respect to its position, m_i is the mass of i atom, and a_i is its acceleration [62]. In the computer simulation of particle models, the time evolution of a system of interacting particles is determined by the integration of the equations of motion. Here, one can follow individual particles to see how they collide, repel each other, attract each other, and how several particles are bound to each other, or are separating from each other. Distances, angles and similar geometric quantities between several particles can also be computed and observed over time. Such measurements allow the computation of relevant macroscopic variables such as kinetic or potential energy, pressure, diffusion constants, transport coefficients, structure factors, spectral density functions, distribution functions, and many more [63]. It doesn't account the electron-electron or phonon-electron interactions. The thermal conductivity of the CNT is dominated by phonon-phonon interactions while considering electronic contribution to the CNT thermal conductivity to be negligible, at all temperatures [12, 29, 34, 36].

3.2 Interatomic Potentials

One of the most prominent factor in any MD calculations is the interatomic potential. The interatomic potential describes the interacting forces between the atoms and has a direct effect on the value of final results of any properties. Thus, it is necessary to get the good results to have an accurate representation of the interactions between the atoms. Potential function defines the interatomic forces and potential energies between the atoms. It is used to describe

the time evolution of bond angles, bond lengths, and torsions, also the non-bonded van der Waal interactions between molecules. The potential function is a collection of mathematical equations and associated constants designed to define molecular geometry and properties of tested structures. The following potentials are used in work.

3.2.1 Tersoff potential

The Tersoff-type potential, is one of the initial methods for treating covalent bonding interactions in computer simulations developed by Tersoff during 1988 to 1989 [58, 64, 65]. The Tersoff model allows the formation and dissociation of covalent bonds during a simulation. It is given by

$$U_{Tersoff} = \frac{1}{2}\sum_{i\neq j} U_R\left(r_{ij}\right) + \frac{1}{2}\sum_{i\neq j} B_{ij} U_A\left(r_{ij}\right)$$

Where U_R and U_A represent repulsive and attractive potentials, B_{ij} is the bond order for the bond between atom *i* and *j*, and r_{ij} is the distance between the two atoms.

3.2.2 REBO potential

Later on, the potential function based on Tersoff's covalent-bonding formalism for hydrocarbons was developed by Brenner [66]. This potential was modified to contain improved analytic functions, and it was named as second-generation reactive empirical bond order (REBO) potential [60]. This potential function was able to produce a more reliable function for predicting bond lengths, energies, and force constants than an earlier version and an improved fit over the bulk elastic properties of diamond.

$$E_{ij}^{REBO} = V_{ij}^{R}(r_{ij}) + b_{ij}\, V_{ij}^{A}(r_{ij}),$$

Where V_{ij}^{R} and V_{ij}^{A} are repulsive and attractive pairwise potentials, determined by the atom types (carbon or hydrogen) of atoms *i* and *j*, and r_{ij} is the distance between the two atoms.

3.2.3 AIREBO potential

Stuart et al. [59] developed the potential based on REBO and introduced non-bonded interactions through an adaptive treatment of the intermolecular interactions (e.g., the intermolecular interaction potential and torsion interaction potential added to second generation REBO from 2002), it is referred as adaptive intermolecular REBO potential (AIREBO) [59]. It is defined as below:

$$E = \sum_i \sum_{j\neq i} (E_{ij}^{REBO} + E_{ij}^{LJ} + \sum_{k\neq i,j} \sum_{l\neq i,j,k} E_{kijl}^{TORSION}),$$

where, E_{ij}^{REBO} is the REBO potential, E_{ij}^{LJ} is the Lennard-Jones potential to define intermolecular interaction, and $E_{kijl}^{TORSION}$ is the torsion interaction potential, and *i*, *j*, k and *l* represent the atoms taken into account for dihedral angle.

3.2.3.1 Lennard-Jones 12-6 potential

The long range Lennard-Jones (LJ) 12-6 potential accounts for the non-bonded interactions between atoms. It is given as:

$$E = 4\varepsilon\left[\left(\frac{\sigma}{r}\right)^{12} - \left(\frac{\sigma}{r}\right)^{6}\right], r < r_c$$

where, r_c is the LJ cut-off radius beyond which van der Waals interaction is negligible and it is taken equal to 2.5 σ and value of σ for C-C = 3.4 A^0. The parameters ε and σ are the coefficients of depth of potential well and equilibrium distance, respectively. Here, the 6th order term dominates at large distances and constitute the attractive part. This is system that gives cohesion to the system. It is originated by dipole-dipole interactions in turn due to fluctuating dipoles. While the 12th order term dominates at short distances, models the repulsion between atoms when they are brought very close to each other [62].

3.2.3.2 Torsion interaction potential

The torsional potential also accounts for nonbonded interactions, introduces torsional interactions. It is defined in the AIREBO model as:

$$E^{tors} = \frac{1}{2}\sum_{i}\sum_{j\neq i}\sum_{k\neq i,j}\sum_{l\neq i,j,k} w_{ij}\,(r_{ij})w_{jk}(r_{jk})w_{kl}(r_{kl}) \times V^{tors}(w_{ijkl})$$

The ususal form for the torsional potential is a cosine power series in the dihedral angle *w*,

$$V = \tfrac{1}{2}\textstyle\sum_{k=1}^{3} V_k[1-(-1)^k\cos(kw)],$$

where, the coefficients V_k are selected for each individual molecule based on relative energies and barriers to rotation and *k* is number of each molecule. In case of chemical reactions occur in molecule, resulting the change in energies and barriers to rotation. The torsional potential with a single minimum is given by:

$$V^{tors}(w) = \in\left[\frac{256}{405}cos^{10}\left(\frac{w}{2}\right) - \frac{1}{10}\right]$$

And ∈ is barrier height.

3.2.4 Optimized Tersoff potential

These Optimized Tersoff Potential [61] parameter sets for the Tersoff and Brenner empirical interatomic potentials represents better lattice thermal conductivities of SWCNTs. It gives an improved representation of the acoustic-phonon dispersions and the anharmonic interatomic force constants.

3.2.5 PCFF

Force field are used to describe the potential energy for the atomistic system. Class I force fields such as DREIDING have particular importance for polymers and versatile in use. However, for the bonded interactions, it only contains the harmonic terms and doesn't include the cross-terms. Class II force fields have been extensively parameterized and consists of both anharmonic and cross-coupling terms to adequately represent the ab-initio potential energy surface (PES). These include the original consistent valence force field (CVFF), and the consistent force field (CFF) developed out of the (CVFF) [30]. PCFF, an ab-initio type force field, includes parameters that are derived from ab-initio data using a least-squares-fit technique given by Hagler and co-workers [57]. Many of the nonbonded parameters, like atomic partial charges and LJ 9-6 parameters, of PCFF are same as in the CFF91 force field. The nonbonded parameters are derived by fitting to molecular crystal data, based on energy minimization calculations [67].

The total steric energy of a molecule for PCFF can be written as a sum of the energies of the interactions:

$$E_{total} = E_{bonds} + E_{angles} + E_{dihedrals} + E_{improper} + E_{cross\ terms} + E_{VdWaals} + E_{Coulomb},$$

Where, E_{bonds} , E_{angles}, $E_{dihedrals}$, $E_{improper}$, $E_{cross\ terms}$, $E_{VdWaals}$ and $E_{Coulomb}$ are the energies corresponding to bond, angle, dihedral, improper, cross terms, van-der Waals and Coulombic interactions, respectively. The bond stretching, angle bending, dihedrals, impropers and cross terms interactions are called bonded interactions because the atoms involved must be directly bonded or non-bonded to a common atom. The van-der Waals and electrostatic interactions are between non-bonded atoms and termed as non-bonded interactions. All the terms are mentioned as below:

Bond Stretching Energy: The bond energy is due to the compression or extension of the bonds between the atoms in the system. The energy is given by the following equation:

$$E_{bonds} = \sum_b [k_2(b - b_0)^2 + k_3(b - b_0)^3 + k_4(b - b_0)^4],$$

where, $k_2, k_3, and\ k_4$ are the parameters for bond stretching, b and b_0 are the current distance and equilibrium distance between two atoms.

Angle Bending Energy: The energy obtained from the angle bending is given by the following equation.

$$E_{angles} = \sum_{\theta}[k_2(\theta - \theta_0)^2 + k_3(\theta - \theta_0)^3 + k_4(\theta - \theta_0)^4],$$

where, $k_2, k_3, and\ k_4$ are the parameters for angle bending, θ and θ_0 are the current angle and equilibrium angle between the bonded atoms, respectively.

Dihedral Energy: The dihedral energy is due to the rotation of bonded atoms, and it is given by the following equation:

$$E_{dihedrals} = \sum_{\varphi}[k_1(1 - \cos\varphi) + k_2(1 - \cos 2\varphi) + k_3(1 - \cos 3\varphi)],$$

where, $k_1, k_2, and\ k_3$ are the fourier series coefficients used for dihedral, and φ is the dihedral angle.

Improper Energy: Improper or out-of-plane potentials are used to describe the interaction of four contiguous atoms. It is defined as below:

$$E_{improper} = \sum_{\varkappa} K\left[\frac{\varkappa_{ijkl} + \varkappa_{ijkl} + \varkappa_{ijkl}}{3} - \varkappa_0\right],$$

where, K is the parameter used for improper potentials, and $\varkappa_{ijkl}, \varkappa_{ijkl}, \varkappa_{ijkl}$ and $\varkappa_0$ are out of plane angle or improper angle.

Cross-terms Energy: These are used to represent the effect of one type of deformation on another, such as bond-bond, bond-angle, bond-torsion, angle-angle, and angle-torsion etc. It contains the cross-terms which are defined as below:

$E_{cross\ terms} = E_{bb} + E_{ba} + E_{aa} + E_{aat} + E_{ebt} + E_{mbt} + E_{bb13} + E_{at},$

$E_{bb} = B(b_{ij} - b_1)(b_{jk} - b_2),$

$E_{ba} = [M_1(b_{ij} - b_1) + M_2\ (b_{jk} - b_2)](\theta - \theta_0),$

$E_{aa} = N_1(\theta_{ijk} - \theta_1)(\theta_{kjl} - \theta_3) + N_2(\theta_{ijk} - \theta_1)(\theta_{ijl} - \theta_2) + N_3(\theta_{ijl} - \theta_2)(\theta_{kjl} - \theta_3),$

$E_{aat} = B'(\theta_{ijk} - \theta_1)(\theta_{jkl} - \theta_2)\cos\varphi,$

$E_{ebt} = (b_{ij} - b_1)[A_1 \cos\varphi + A_2 \cos 2\varphi + A_3 \cos 3\varphi] + (b_{kl} - b_3)[C_1 \cos\varphi + C_2 \cos 2\varphi + C_3 \cos 3\varphi]$,

$E_{mbt} = (b_{jk} - b_2)[B_1 \cos\varphi + B_2 \cos 2\varphi + B_3 \cos 3\varphi]$,

$E_{bb13} = B^1(b_{ij} - b_1)(b_{kl} - b_3)$, and

$E_{at} = (\theta_{ijk} - \theta_1)[D_1 \cos\varphi + D_2 \cos 2\varphi + D_3 \cos 3\varphi] + (\theta_{jkl} - \theta_2)[E_1 \cos\varphi + E_2 \cos 2\varphi + E_3 \cos 3\varphi]$,

where,

E_{bb} : Bond-bond Energy, E_{ba} : Bond-angle Energy; E_{aa} : Angle-angle Energy; E_{aat} : Angle-angle-torsion Energy; E_{ebt} : End-bond-torsion Energy; E_{mbt} : Middle-bond-torsion Energy; E_{bb13} : Bond-bond 13 Energy; E_{at} : Angle-torsion Energy.

Further, *B*, and M_1 and M_2 are the constants corresponding to bond-bond energy and bond-angle energy. b_{ij}, b_{jk}, b_{kl} are the distances between the atoms *i* and *j*, *j* and *k*, and *k* and *l*, respectively. b_1, $b_2$and b_3 are equilibrium bond lengths for pairwise interactions. θ and θ_0 are the current angle and equilibrium angle between three atoms. N_1, N_2, N_3 are the constants corresponding to angle-angle energy, and and B' is for angle-angle-torsion energy. $\theta_{ijk}, \theta_{jkl}$, $and\ \theta_{ijl}$ are the angle between three atoms (i.e., *i*,*j*,*k*, *j*,*k*,*l*, and i,*j*,*l*). $\theta_1, \theta_2, and\ \theta_3$ are the equilibrium angles. φ is dihedral angle. A_i, C_i are the constants for end-bond-torsion energy, and B_i is the constant for middle-bond-trosion energy, with i = 1, 2, 3. B^1 is the constant corresponding to bond-bond13 energy, and D_i, E_j are the constants for angle-torsion energy.

Van der Waals: It is non-bonded interactions between two atoms. It is represented by LJ potentials, and given as below:

$$E_{vdWaals} = \sum_{i,j} \epsilon_{ij} \left[2 \left(\frac{r_{ij}^0}{r_{ij}} \right)^9 - 3 \left(\frac{r_{ij}^0}{r_{ij}} \right)^6 \right],$$

where, ϵ_{ij} and r_{ij} are LJ parameters, obtained using the combination rule for individual atom. 6th term and 9th terms are used to represent interactions for the long-range and short-range between the atoms, respectively.

Coulomb Energy: This potential is used to represent the coulombic interactions between the atoms. It is defind as below:

$$E_{Coulomb} = \sum_{i,j} \frac{q_i q_j}{r_{ij}},$$

where, q_i and q_j are the charges on atoms i and j, and r_{ij} is the distance between these two atoms [30].

3.3 Ensembles

Ensemble refers to a collection of all atoms that has same thermodynamic property. Ensembles are categorized into four categories, which represents the specific thermodynamic state for the atomistic system.

NVE

This ensemble is called as Microcanonical ensemble, in which number of atoms (N), volume (V), and energy (E) remain constant. This type of ensemble describes an isolated system.

NVT

This ensemble is called as Canonical ensemble, in which number of atoms (N), volume (V) and temperature (T) remain constant.

NPT

This ensemble is called as Isobaric-isothermal ensemble, in which number of atoms (N), pressure (P) and temperature (T) remain constant.

NPH

This ensemble is called as Isoenthalpic-isobaric ensemble, in which number of atoms (N), pressure (P) and enthalpy remain constant [1].

Chapter 4

4 Simulation Methods

4.1 NEMD vs EMD

There are two types of MD methods for finding the thermal conductivity that can be classified as (i) EMD, and (ii) NEMD. EMD is based on Green-Kubo formula derived through linear response theory that involves the time integration of heat current correlation functions [17]. EMD method can calculate the thermal conductivity along all directions in one simulation, but is computationally more expensive [68]. In the NEMD method, NEMD can calculate the thermal conductivity only in one direction, and it is computationaly less expensive [68]. The The thermal conductivity is calculated using the Fourier law that can be achieved into two ways. One way is to impose the temperature gradient and calculate the heat flux while other involves imposing the heat flux, and then calculate the temperature gradient [27].

4.2 Models Preparation

In this work, atomistic structures were modelled using Material Studio 8.0 [69]. The (10,10) armchair SWCNTs were prepared within the length range between 10 to 1000 nm. To check the temperature dependence of SWCNTs, two armchair SWCNTs with chirality (14,14) and (10,10) and one zig-zag SWCNTs with chirality (24,0) of length 250 nm were modelled. The chain length of polyethylene polymer is made up of ethylene monomers or repeat units. To find the chain length effect of the polyethylene polymer, the chain length with different number of repeat units (i.e., 10, 50, 100, 150 and 200) were prepared. To investigate the functionalization effect on nanocomposites, -COOH functional group was used. First, a (5,5) armchair SWCNT was prepared having the length of 51.2 A^0, and the -COOH functional group was attached to 1%, 3% and 5% of carbon atoms on the outer surface of the CNTs. Thereafter, both unfunctionalized and functionalized SWCNTs were reinforced in to the polyethylene polymer matrix, having chain length of 200 repeat units, into the simulation box of size $50A^0 \times 50A^0 \times 51.2A^0$, and the atoms of polymers were adjusted to give the final bulk density equivalent to the experimental density of 0.95 g/cm^3. The same procedure was employed for the neat polyethylene polymer with the different chain lengths.

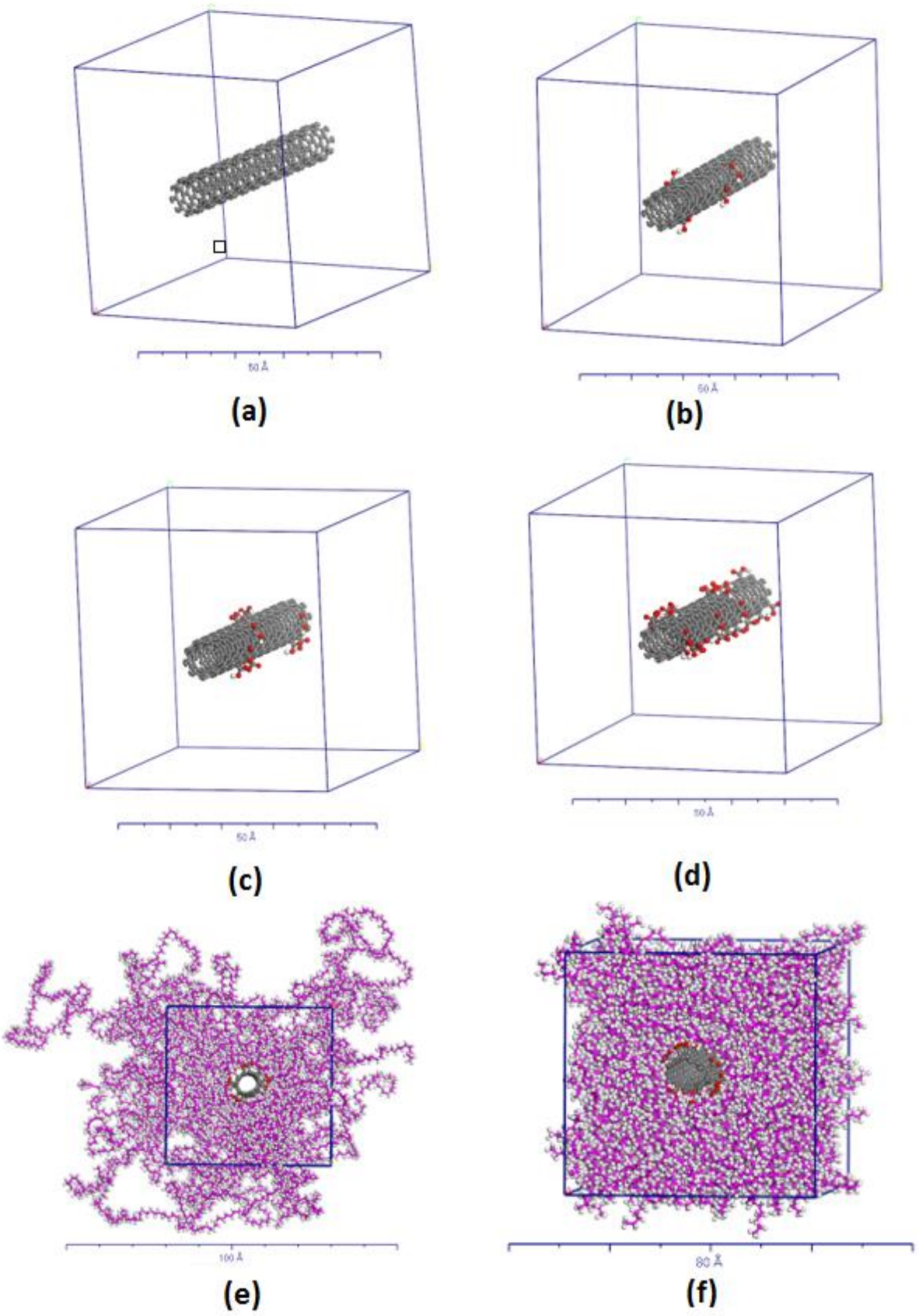

Fig. 1. (5,5) SWCNT (a) without functionalization, and (b) with 1% functionalization, (c) with 3% functionalization, and (d) with 5% functionalization of carbon atoms in a simulation box of size $50A^0 \times 50A^0 \times 51.2A^0$; (e) Packing of polyethylene polymer chain around the fuctionalized SWCNT in a simulation box of size $50A^0 \times 50A^0 \times 51.2A^0$, and (f) Compressed simulation box to get the desired density.

After preparing the structures, Large-scale Atomic/Molecular Massively Parallel Simulator (LAMMPS) [70] package was used to perform the simulations. Equilibrium procedure carried out was same for polymer and nanocomposite. After initial packing, the density of polymer and nanocomposites were nearer to 8% of the bulk density of 0.95 g/cm^3. To achieve the desired density of 0.95 g/cm^3, first, energy minimization of the system was done at 100 K and timestep was taken as 0.25 fs. After a Langevin thermostat was used to maintain the system at 100 K with a damping constant of 100 fs, the structure was deformed to achieve requisite density in number of steps, and minimization of structure was performed simultaneously. Using NVT-MD simulation, thermal annealing was carried out to find the global minima or lowest potential energy state. Atomistic system was heated with a rate of 0.02 K/fs from 100 to 1000 K, equilibrating at 1000 K for 50 ps, and then cooling to 300 K with same rate of 0.02K/fs. This annealing procedure was performed once again to make sure to have the lowest energy state of the system. After that the system was allowed to equilibrate at 300 K for 50 ps. Then using the NPT-MD simulation, the pressure was increased from 1 to 100 atm at 300 K within 10 ps and allowed to 100 atm at 300 K for another 50 ps, followed by compression to 1 atm at 300 K for 10 ps, and equilibrated at 300 K for 500 ps. The bulk density was 20% lower than the experimental polyethylene density 0.95 g/cm^3. However, in our all simulations, the bulk density was maintained at 0.95 g/cm^3 to match the results with observed results of HDPE polymer [22, 38] and this maintained bulk density, named as desired density (i.e., 0.95 g/cm^3). In the case of neat polyethylene polymers, the bulk density obtained using the NPT-MD simulations that was 20% lower than desired density, named as equilibrium density (0.76 g/cm^3).

4.3 Computational Details

4.3.1 General Procedure

Classical RNEMD was used to calculate the thermal conductivity with periodic boundary conditions in all directions. Using the Muller-Plathe method [71], the heat flux was imposed, and the temperature gradient was obtained as the system response [36].

To impose the heat flux over the system, the whole system was divided into 20 slabs along the desired direction, 1st slab and the 11th slab are designated as cold and hot slab. Then, one pair of atoms, the hottest atom from the cold slab and the coldest atom from the hot slab, are selected and enforced to swap its kinetic energy at desired timesteps. This swapping of kinetic energy

continuous over a period of time, and induce the temperature gradient in the system, and the heat flux is written as:

$$q_z = \frac{\sum_{i=1}^{h} \frac{1}{2} m_i ({v_{h_i}}^2 - {v_{c_i}}^2)}{2A_c t},$$

where, q_z is the heat flux in the *z* direction, *m* is the mass of the atoms, A_c is the cross-sectional area which is equal to πdt, *d* is the mean diameter of the CNT and *t* is thickness of the CNT taken as 0.34 nm, v_h and v_c are the velocities of the hot and cold atoms, respectively, *t* is taken as time in the simulation and *h* refers to the number of transfers. As it can be seen in Fig. 2 that energy can flow in both directions for the periodic conditions, therefore, the factor of 2 is considered in the denominator.

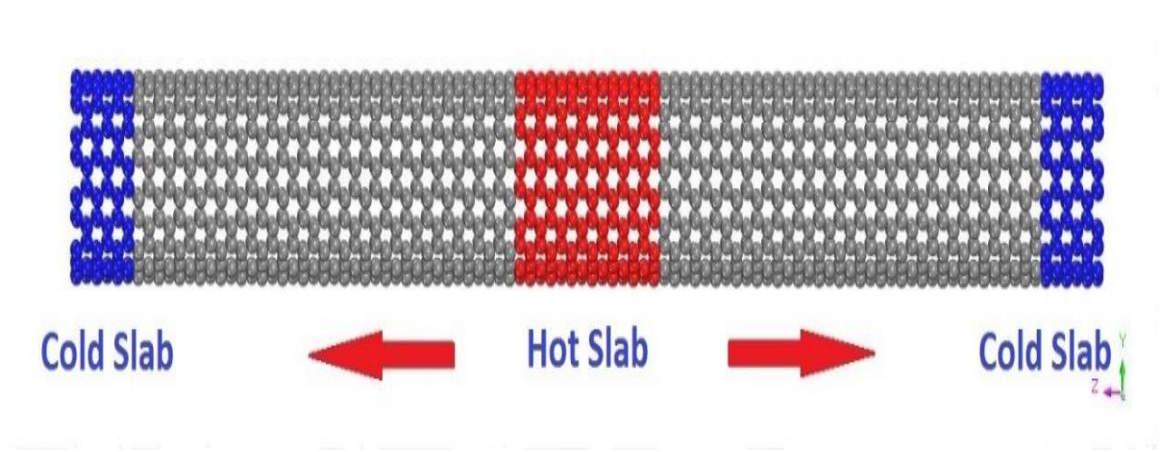

Fig. 2. The direction of heat flux in both directions.

While to get the temperature profile, the whole system was divided into the 50 slabs. And temperature of each slab is calculated from the equipartition theorem given as:

$$T_j = \frac{1}{3N_s K_B} \sum_{l \epsilon S_j} m_l v_l^2.$$

Here, T_j is the temperature of *j*th slab, N_s is the number of atoms in the *j*th slab, K_B is the Boltzmann constant, m_l is the atomic mass, v_l is the instantaneous velocity of atom l, and the summation is performed over atoms contained in the slab *j*. After reaching steady state, the energy transfer imposed by the unphysical velocity exchange is exactly balanced by the heat flux in the opposite direction affected by the thermal conductivity of the system. Fig. 3. Shows the temperature gradient for the (10,10) SWCNT with the length of 1000 nm at different timesteps and at the time step corresponding to steady state (i.e., at 1 ns).

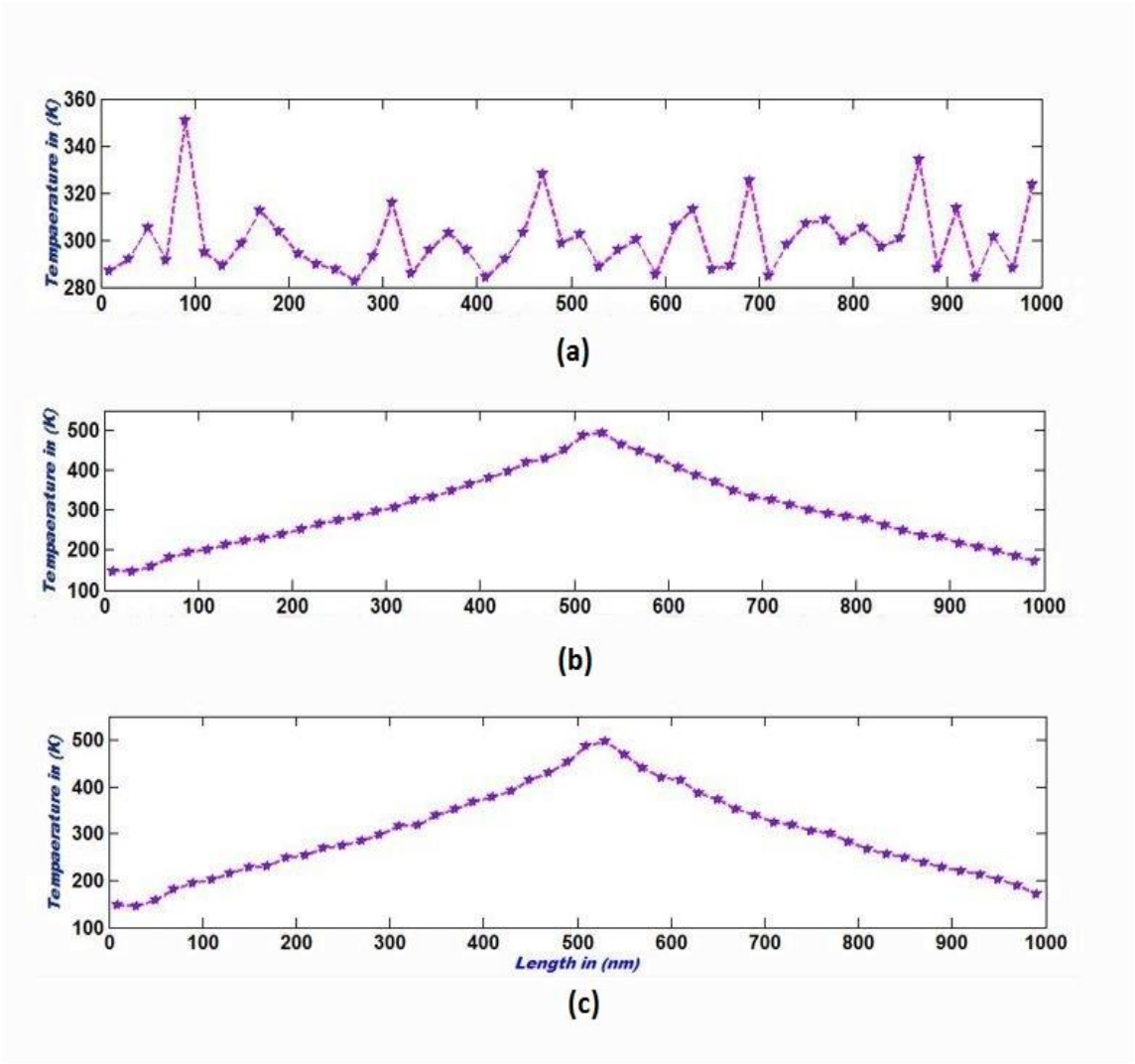

Fig. 3. Temperature profile along the length of CNT at different timesteps (a) at 100000-timesteps, (b) at 1000000-timesteps, (c) at 2000000-timesteps.

The average temperature gradient is found by linear regression of the temperature of the slabs, which shows the linear variation of temperature with the distance. After getting a linear response, simulation is run for another time period to get the thermal conductivity using the Fourier's Law:

$$k = \frac{q_z}{\frac{\partial T}{\partial z}}.$$

4.3.2 Simulation Details for SWCNT

All the MD simulations were carried out with the Large-scale Atomic/Molecular Massively Parallel Simulator (LAMMPS) [70]. The interactions between the carbon atoms were modelled by AIREBO potential. Classical equations of motion for each atom were numerically integrated

in time using the velocity Verlet algorithm, which has excellent energy conservation property [18]. In case of SWCNTs, 1 fs time step was used. First, the whole system was equilibrated at 300 K within the NVT ensemble for 100 ps. Then the heat flux was imposed by swapping their kinetic energies once for every 0.01 ps within the NVE ensemble. Simulations were run to equilibrate for 1ns to get the linear response of the temperature gradient. Data were recorded at every one ps time period to get the thermal gradient. Simulations were run for another 1 ns to calculate the average thermal conductivity. All the simulations set up was same for the all other CNTs.

4.3.3 Simulation details for polymers and nanocomposites

In case of polymers and nanocomposites, PCFF [57] force-field was used as potential. A 0.1 fs time step was used. Area of the deformed simulation box perpendicular to the longitudinal axis of the CNT were considered in the calculations to find the thermal conductivity. After the equilibrium procedure as mentioned in Section 4.2, the whole system was equilibrated at requisite temperature within the NVT ensemble for 200 ps. Then the heat flux was imposed for 500 ps to get the linear response of the temperature gradient. Data were recorded every 0.1 ps. Simulations were run for another 500 ps to calculate the average thermal conductivity.

4.4 Validation

To validate the procedure for finding the thermal conductivity, the results were compard with the results predicted by Padgett and Brenner [16] and Salaway and Zhigilei [27]. The simulations were performed for the lengths ranging from 10 nm to 1000 nm for the (10,10) armchair CNT using REBO [60] and AIREBO [59] potentials. Both Padgett and Brenner[16] and Salaway and Zhigilei [27] used the NEMD method to find out the thermal conductivity of CNT. Padgett and Brenner [16] used the Muller-Plathe method [71] with the REBO [60] potential, whereas Salaway and Zhigilei [27] used the Langevin thermostat method with AIREBO [59] potential. In the present study, the Muller plathe method was used with different potentials. To compare the results with the Padgett and Brenner [16], the REBO [60] potential was used, while AIREBO [59] potential was used to compare the results with Salaway and Zhigilei [27]. Fig. 4. shows that the simulation procedure followed in the present study gave the similar results as reported by Padgett & Brenner [16] but showed the gradually increasing trend of thermal conductivity with increasing the length. The comparision of results of present study with Salaway and Zhiglei [27] in Fig. 4 also shows a reasonable agreement.

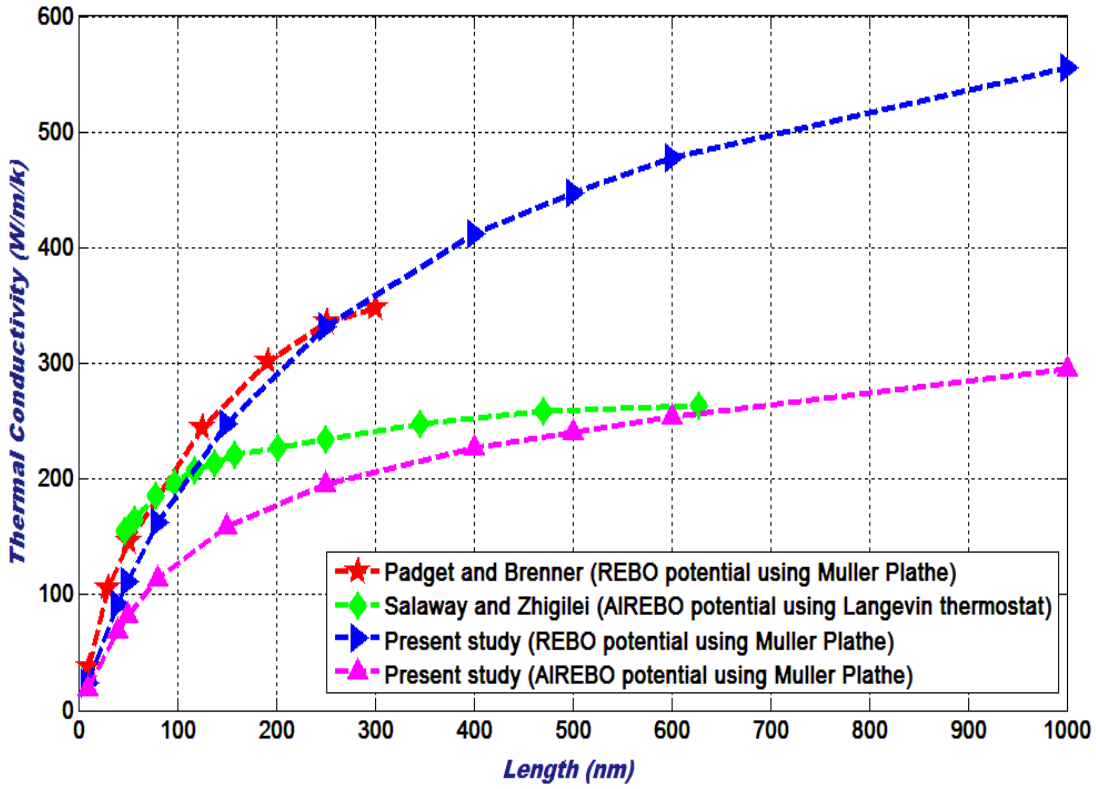

Fig. 4. Thermal conductivity value for different potentials to compare our results.

Chapter 5

5 Results and Discussions

In the first section of this chapter, to find the effect of interatomic potentials, the thermal conductivity of CNTs within the range of lengths 10 - 1000 nm were calculated using different potentials. To investigate the effect of temperature on the thermal conductivity of CNTs with different chirality but at the same length, the temperature was varied from 100 – 700 K using optimized Tersoff potential. Later, in the next section, the chain length was varied from 10 – 200 monomers, to find the effect of chain length on the thermal conductivity of polyethylene polymer for desired and equilibrated density models. To predict the effect of temperature on the thermal conductivity of polyethylene polymer for desired density at different chain length, the temperature was varied from 275 to 350 K. In the last section of this chapter, effect of functionalization on the thermal conductivity of SWCNT/polyethylene nanocomposites was investigated by functionalizing different percentages (i.e., 1%, 3%, 5%) of carbon atoms of SWCNT with –COOH functional group and subsequently, reinforcing the same in polyethylene polymer matrix, made by chain length of 200 monomers. Also, simulations were carried out to find the temperature dependence of functionalized –COOH with SWCNT/polyethylene nanocomposites at the different temperature (i.e. 275, 300, 325 and 350 K).

5.1 Thermal Conductivity of CNT

The valuse of thermal conductivity of CNTs are calculated for different lengths using the optimized Tersoff potential [61]. Later on, the effect of interatomic potential on thermal conductivity of an armchair (10, 10) CNT of length taken in the range 10 – 1000 nm for different potentials, namely Tersoff[58], AIREBO and REBO[60]. Thereafter, the effect of temperature on the thermal conductivity of CNTs of different chirality [i.e., (10,10), (17,0) and (14,14)] was studied for a CNT-length of 250 nm.

5.1.1 Effect of interatomic potential

The results obtained to study the effect of interatomic potential on the thermal conductivity of the CNT are plotted in Fig. 5 and it is observed that the thermal conductivity of CNTs for Optimized Tersoff potential was the highest among all the interatomic potentials. The reason behind this is that major contribution to the thermal conductivities of CNTs are from the acoustic phonons [36], and the optimzed Tersoff potential provides an improved representation of the acoustic-phonon dispersions and the anharmonic interatomic force constants, over all other potentials [20, 61]. The thermal conductivity obtained using the optimized Tersoff potential [61] is also found closer to the experimental results [9] than all other potentials. The convergence of thermal conductivity of CNTs is not achieved up to 1000 nm length for all the interatomic potentials. The increasing trend of thermal conductivity is observed from AIREBO to REBO, REBO to Tersoff, and Tersoff to optimized Tersoff, up to the CNT's length 500 nm. For the lengths greater than 500 nm, the increasing trend was observed from AIREBO to Tersoff, Tersoff to REBO, and REBO to optimized Tersoff potential. For lengths shorter than 200 nm, the strong dependence of the thermal conductivity is found for all the potentials, which suggests the existence of ballistic region [16, 20, 27, 28]. For the lengths greater than 200 nm, the weak dependence of thermal conductivity confirms the transition from ballistic region to diffusive-ballistic region. The difference in thermal conductivity is found to be very small for lengths shorter than 50 nm for the different potentials, which becomes significant for lengths greater than 50 nm. The value of thermal conductivity for optimized Tersoff potential was 1.88 times for AIREBO potential at the length 80 nm which increased to 3.82 times for the length of 1000 nm. The thermal conductivity value obtained in the MD simulation for REBO potential is less than the Tersoff potential up to the length 500 nm, and after that becomes larger than Tersoff potential. However, the difference between the REBO and Tersoff potential was found to be negligible at all the lengths. Therefore, it can be concluded that the results obtained by these two potentials should not differ by more than a small amount.

.

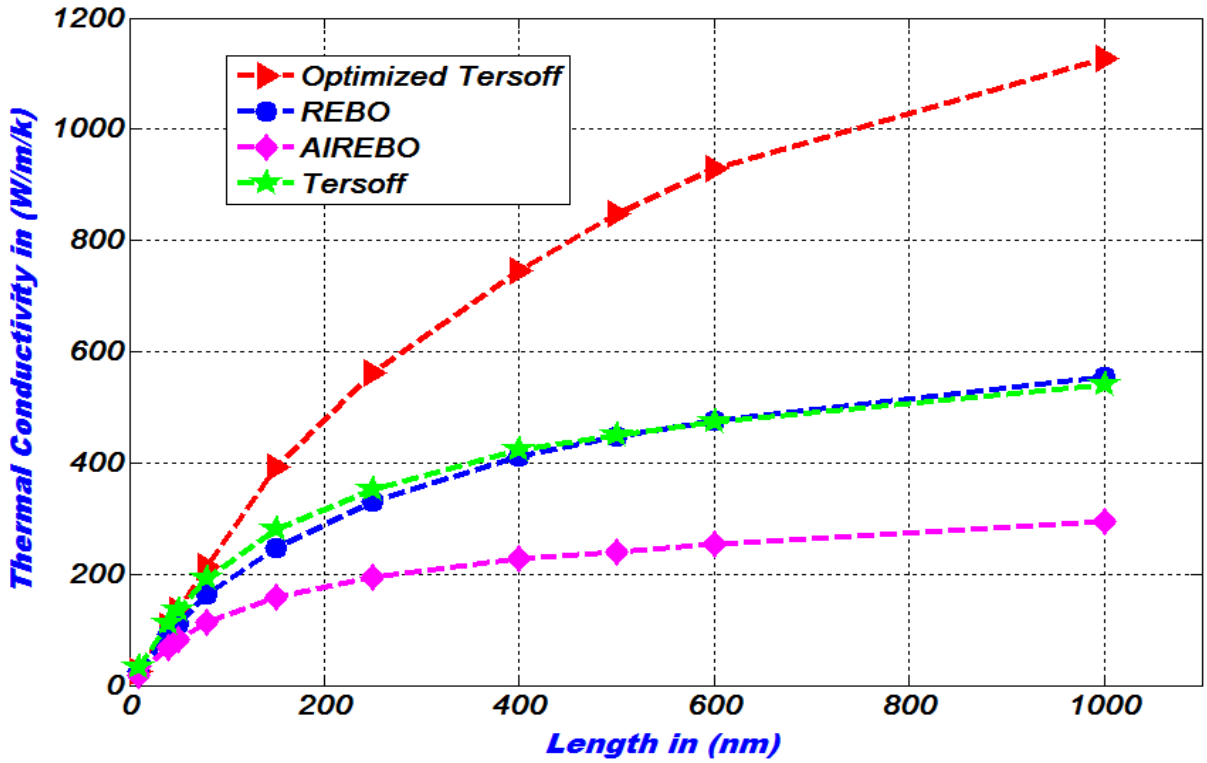

Fig. 5. Thermal conductivity value for four different potentials.

5.1.2 Effect of temperature

Fig. 6 plots the effect of temperature on the thermal conductivity of CNTs of different chirality [i.e., (10,10), (17,0) and (14,14)] for a CNT-length of 250 nm. The results are obtained using Optimized Tersoff potential [61]. It can be seen from Fig. 6 that for all CNTs, the thermal conductivity was found to decrease with the increase in temperature. This can be explained because of the reason that with the increase in temperature, the strong phonon-phonon umklapp scattering becomes dominant which reduces the phonon MFP to further result in decrease in the thermal conductivity. This observation is in good concurrence with the similar observations reported in Refs. [11, 18]. Further, Fig. 6 also shows that the thermal conductivity of armchair (10,10) CNT was higher than the zig-zag (24,0) CNT, having almost the same diameter. It can be noted that the difference in thermal conductivity between CNTs of different chrialities decreases as the temperature increases. Also, it can also seen in Fig. 6 that for armchair CNT of different chiralities, there is no much difference in their thermal conductivity.

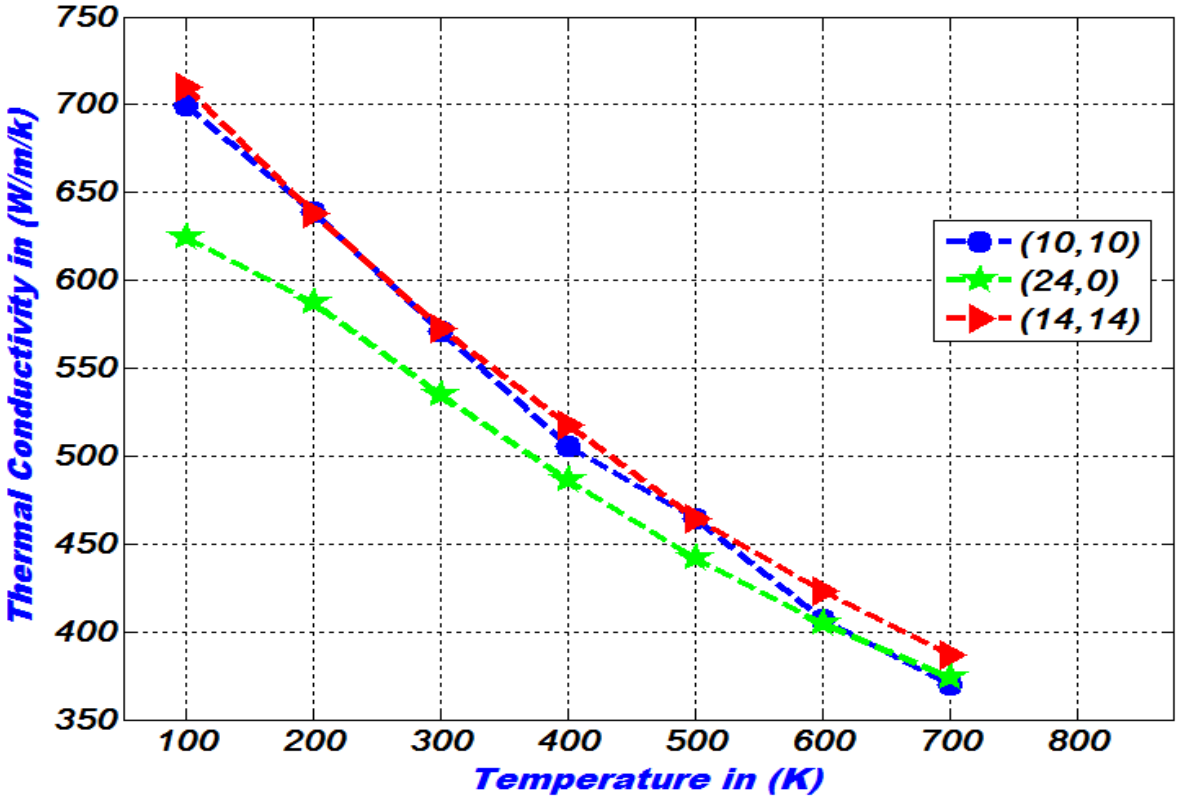

Fig. 6. Thermal conductivity of SWCNTs at different temperatures.

5.2 Thermal Conductivity of Polymer

In this section, the thermal conductivity of polyethylene made of different chain lengths is calculated. To study the effect of chain length of polymer on its thermal conductivity, the chain length is varied from 10 to 200 monomers. Subsequently, the effect of temperature dependence on the thermal conductivity of polymer is investigated.

5.2.1 Effect of chain length

To study the effect of chain length of polyethylene polymer on its thermal conductivity, RNEMD simulations are performed using PCFF [57] while applying using periodic boundary conditions. MD Simulations are performed for both desired and equilibrated density . As seen in Fig. 7, the results show the increase in the thermal conductivity of polyethylene polymer with the increase in the chain length for both desired density and equilibrium density. And the thermal conductivity of desired density (0.95 g/cm^3) is observed higher than the equilibrium density (0.76 g/cm^3) at all the different chain length of the polyethylene polymer. The thermal conductivity for polyethylene polymer is found to vary from 0.337 W/m/k to 0.4273 W/m/k

and 0.117 W/m/k to .2814 W/m/k for desired density and equilibrated density, when the chain lengths are varied from 10 – 200 monomers. The results show the enhancement in the percentage of thermal conductivity with increase in the chain lengths from 10 to 200 monomers of polyethylene polymers by 26.68 % and 58.31 % for the desired and equilibrium density.

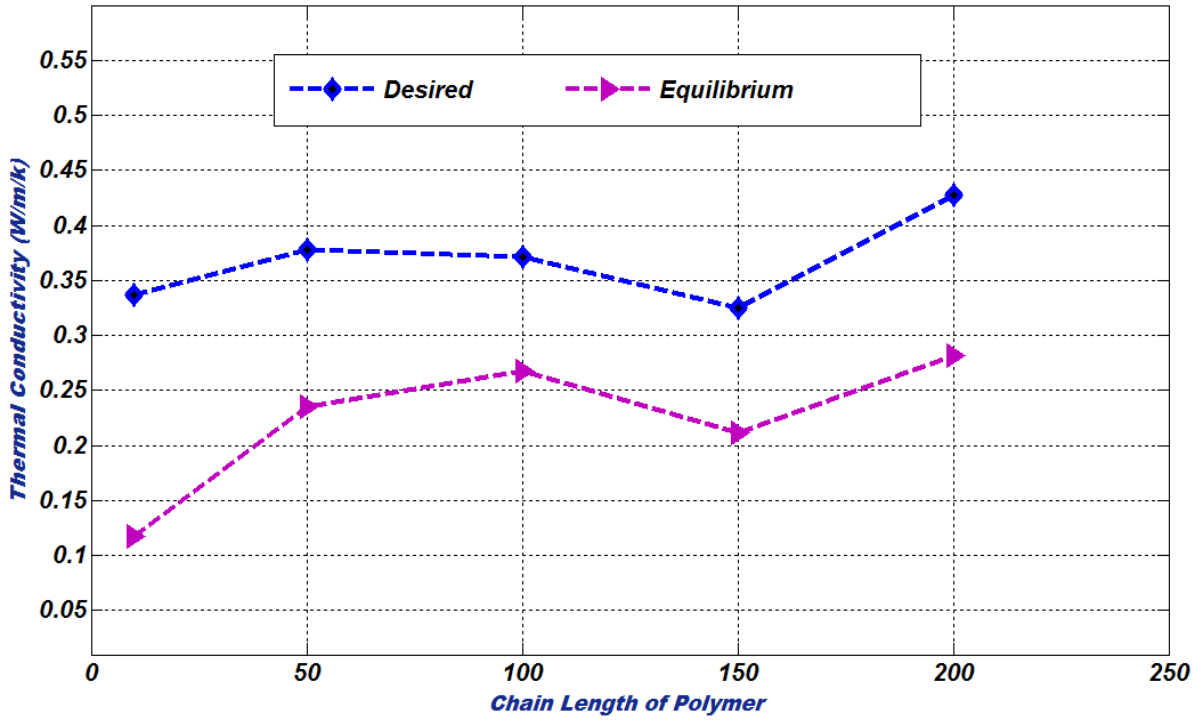

Fig. 7. Effect of chain length on the thermal conductivity of polyethylene polymers at desired and equilibrium density.

5.2.2 Effect of temperature

To investigate the effect of the temperature on different chain lengths of polyethylene polymer, RNEMD simulations were performed on the desired polyethylene polymer with different chain lengths from 10 – 200 monomers within the temperature range of 275 to 350 K. The thermal conductivity of polyethylene polymer with different chain length at different temperature (i.e., 275 – 350 K) is plotted in Fig. 8. The enhancement of thermal conductivity of polyethylene polymer at different chain length is observed with increase in the temperature. The results observed in this study show the same increasing trend as observed in [42]. The thermal conductivity in terms of percentage is observed with the increment of 13% more for the individual's chain length when the temperature increased from 275 to 325 K.

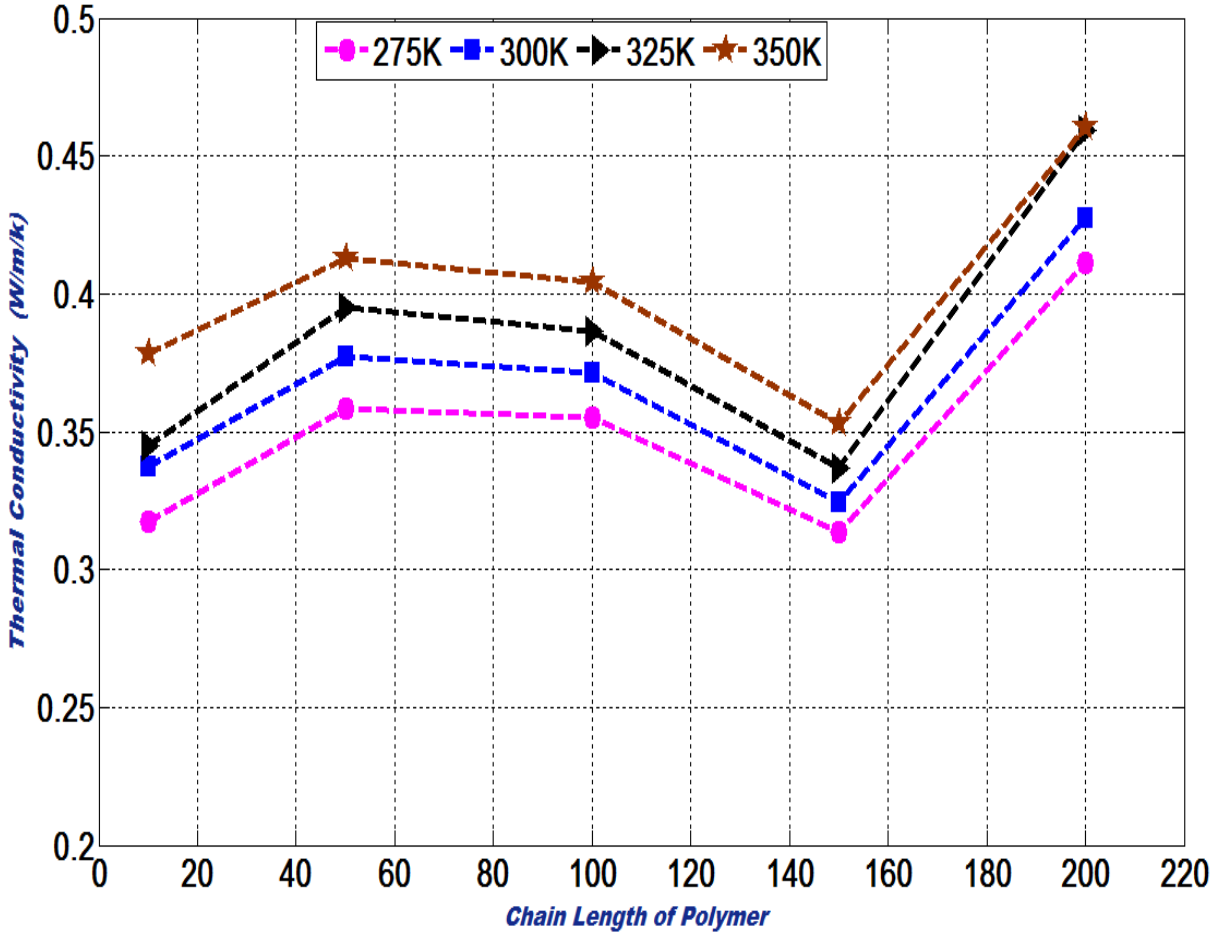

Fig. 8. Effect of temperature at different chain length on the thermal conductivity of polyethylene polymers at desired density.

5.3 Thermal Conductivity of Functionalized Nanocomposites

MD simulations are performed with different percentages of the functional group (i.e. 1%, 3%, and 5%) of carbon atoms attached to the outer surface of the CNTs, to investigate the effect of -COOH functional group on the thermal conductivity of SWCNT/polyethylene nanocomposites, Later on, MD simulations are carried out to find the effect of the temperature dependence of -COOH functionalized SWCNT/polyethylene nanocomposites at the different temperature (i.e. 275, 300, 325 and 350 K).

5.3.1 Effect of functionalization

RNEMD simulations are performed using PCFF to investigate the effect of functionalization on the thermal conductivity of nanocomposites, at 300 K. Fig. 9 plots the effect of –COOH functional group on the thermal conductivity of SWCNT/polyethylene nanocomposites. The results shows that the thermal conductivity of SWCNT/polyethylene nanocomposites is found to be low as compared to neat polyethylene nanocomposites. Further upon the functionalization

of 1% and, 1% to 3%, the thermal conductivity of -COOH functionalized SWCNT/polyethylene nanocomposites is found to decrease.When functionalization is increased to 5% carbon atoms with –COOH functional group, the thermal conductivity of functionalized SWCNT/polyethylene nanocomposites is increased.

However, the CNTs have excellent intrinsic thermal conductivity [54], the thermal conductivity of SWCNT/polyethylene nanocomposites without the functional group is found to be lower than the neat polyethylene polymer. The reason behind is that due to the presence of the interfacial thermal resistance which acts as a barrier to the heat flow resulting from differences in the phonon spectra of the SWCNT and the polymeric polyethylene matrix as discussed in Refs. [22, 53, 54]. When 1% -COOH functional group attached to the outer surface of the SWCNTs, the thermal conductivity is observed to decrease as compared to unfunctionalized SWCNT/polyethylene nanocomposites, and for 3% SWCNT-COOH, further decrement in the thermal conductivity is observed . However, on the addition of 5% -COOH functional group to the SWCNT, the thermal conductivity is enhanced and found to be even greater than the unfunctionalized SWCNT/polyethylene nanocomposites. This can be explained by two phenomena occurs in SWCNT/polymer nanocomposites upon increasing the functionalization, the SWCNT coupling to the polyethylene matrix increases with the increase of the degree of functionalization. However, it also create defects in the CNTs as functionalization leads to change the sp^2 bonds to sp^3 bonds, which results in the increase of sp^3 bonded carbon atoms in the nanotubes. This conversion creates scattering centers for acoustic phonon propagating along the CNT, reduces the MFP of the phonons, which ultimately reduces the thermal conductivity of the CNTs. These observations are in good concurrence with the similar observations reported in Ref. [54]. The outcome of this study is that with the increase in functionalization, the coupling between the SWCNT and the polyethylene matrix increases and dominant over the defects created by the functionalization of the CNTs leads to the increase in the thermal conductivity of functionalized SWCNT/polyethylene nanocomposites by allowing the transfer of phonons between the CNTs and the polymer matrix.

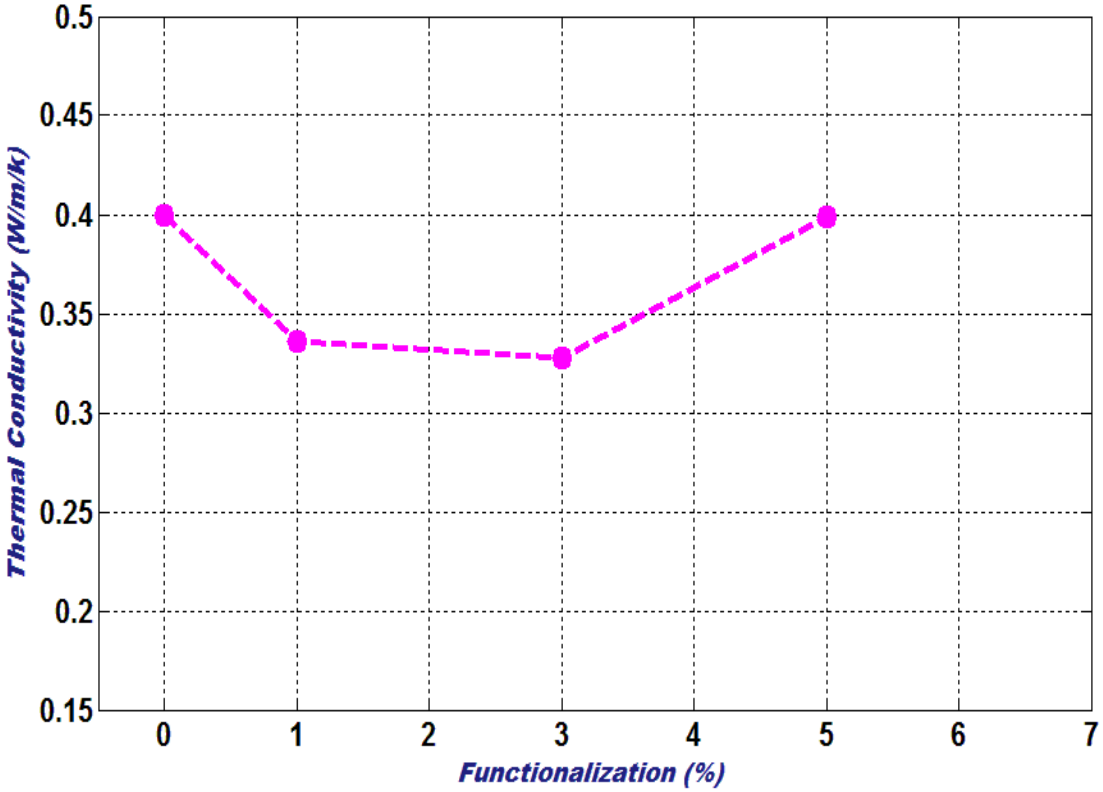

Fig. 9. Functionalization effect of (-COOH) group at different % of carbon atoms on the thermal conductivity of functionalized SWCNT/polyethylene polymers at desired density at 300 K.

5.3.2 Effect of temperature

RNEMD simulations are performed at different temperature (i.e. 275, 300, 325 and 350 K) using PCFF to investigate the temperature dependence for both unfunctionalized and functionalized SWCNT/nanocomposites. Fig. 10 plots the effect of temperature of (-COOH) functional group at different % of carbon atoms on the thermal conductivity of functionalized SWCNT/polyethylene polymers at desired density. The results suggest that the thermal conductivities for both unfunctionalized and functionalized SWCNT/polyethylene nanocomposites are increased with the increase of the temperature. The linear increasing trend of thermal conductivity is observed upon increasing the functionalization for SWCNT-COOH/polyethylene nanocomposites.

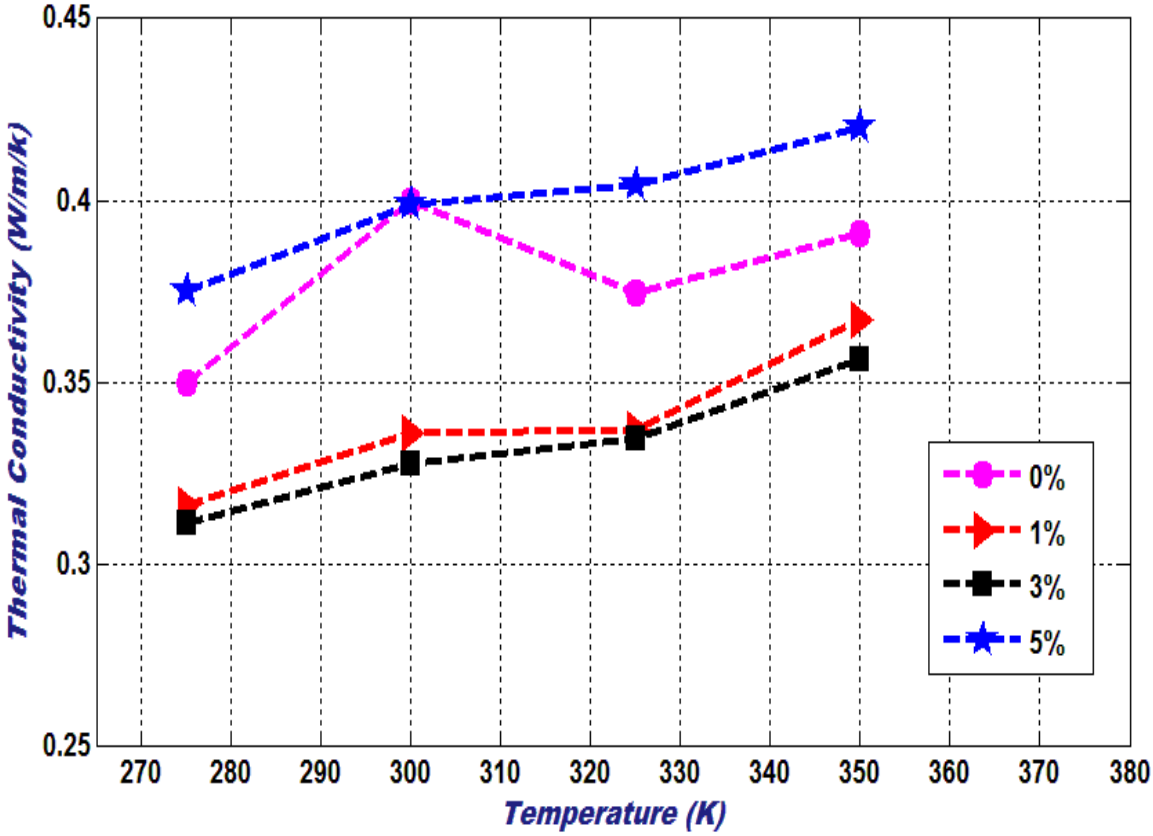

Fig. 10. Effect of temperature of (-COOH) functional group at different % of carbon atoms on the thermal conductivity of functionalized SWCNT/polyethylene polymers at desired density.

Chapter 6

6 Conclusions & Future Work

6.1 Conclusions

RNEMD simulations were carried out to find the effect of interatomic potentials on thermal conductivity of the (10,10) armchair SWCNTs with the increase of lengths using periodic boundary conditions in all directions. The strong dependency of thermal conductivity i.e., ballistic thermal transport was observed up to the length of 200 nm for all the interatomic potentials. Transition ballistic-diffusive regime was found for the lengths greater than 200 nm where the weak dependency of thermal conductivity was observed. The convergence was not achieved up to 1000 nm length for all interatomic potentials. The difference in thermal conductivity was found to be very small for the lengths shorter than 50 nm for the different potentials. For the length greater than 50 nm, a significant difference was found. The thermal conductivity value for Optimized Tersoff potential was 1.88 times for AIREBO potential at the length 80 nm which increased to 3.82 times at the length 1000 nm. To know the temperature dependence of thermal conductivity, Simulations were performed on (10,10), (24,0) and (14,14) SWCNTs with identical lengths and computational set up using optimized Tersoff. The difference in thermal conductivity between CNTs decreases as temperature increases. The result shows that thermal conductivity value for all the CNTs become negligible at higher temperatures.

For polyethylene polymers, the thermal conductivity for polyethylene polymer was found to vary from 0.337 W/m/k to 0.4273 W/m/k and 0.117 W/m/k to .2814 W/m/k for desired density and equilibrated density, when the chain lengths were varied from 10 – 200 monomers. The results showed the enhancement in the percentage of thermal conductivity with increase in the chain lengths from 10 to 200 monomers of polyethylene polymers by 26.68 % and 58.31 % for the desired and equilibrium density. To investigate the effect of the temperature on different chain lengths of polyethylene polymer, the thermal conductivity in terms of percentage was observed with the increment of 13% more for the individual's chain length when the temperature was increased from 275 to 325 K. In case of investigating the effect of functionalization on the thermal conductivity of nanocomposites, the study shows that with the

increase in functionalization, the coupling between the SWCNT and the polyethylene matrix increases and dominant over the defects created by the functionalization of the CNTs leads to the increase in the thermal conductivity of functionalized SWCNT/polyethylene nanocomposites by allowing the transfer of phonons between the CNTs and the polymer matrix. Simulations were also performed at different temperature (i.e. 275, 300, 325 and 350 K) using PCFF to investigate the temperature dependence for both unfunctionalized and functionalized SWCNT/nanocomposites. The linear increasing trend of thermal conductivity was observed upon increasing the functionalization for SWCNT-COOH/polyethylene nanocomposites.

6.2 Future Work

In the present work, the effect of -COOH functional group was studied on the role of interfacial thermal resistance of SWCNT/polyethylene nanocomposites. The COOH-SWCNT shows the enhancement in thermal conductivity of nanocomposites. But the key point that exists, how vital is the use of functional group on the enhancement of thermal conductivity of nanocomposites. In the present study, the pure polymer chain length were considered. The further work can be study by including the crosslinking between the polymers or polymers and functional group, which is more realistic model.

7 References

[1] Lim MCG, Zhong Z. Carbon Nanotubes as Nanodelivery Systems: An Insight Through Molecular Dynamics Simulations. Springer Science & Business Media; 2013.

[2] Iijima S. Helical microtubes of graphite carbon. Nature 1991;354:56–8.

[3] Iijima S, Ichihashi T. Single-shell carbon nanotubes of 1-nm diameter. Nature 1993;363:603–5.

[4] Bethune DS, Kiang CH, Vries MS De, Gorman G, Savoy R, Vazquez J, et al. Cobalt-catalysed growth of carbon nanotubes with single-atomic-layer walls. Nature 1993;363:605–7.

[5] Ruoff RS, Lorents DC. Mechanical and thermal properties of carbon nanotubes. Carbon N Y 1995;33:925–30. doi:10.1016/0008-6223(95)00021-5.

[6] Sawaya S, Akita S, Nakayama Y. Correlation between the mechanical and electrical properties of carbon nanotubes. Nanotechnology 2007;18:35702.

[7] Wu Y, Huang M, Wang F, Huang XMH, Rosenblatt S, Huang L, et al. Determination of the Young's modulus of structurally defined carbon nanotubes. Nano Lett 2008;8:4158–61.

[8] Li T, Tang Z, Huang Z, Yu J. A comparison between the mechanical and thermal properties of single-walled carbon nanotubes and boron nitride nanotubes. Phys E Low-Dimensional Syst Nanostructures 2017;85:137–42. doi:10.1016/j.physe.2016.08.012.

[9] Pop E, Mann D, Wang Q, Goodson K, Dai H. Thermal conductance of an individual single-wall carbon nanotube above room temperature. Nano Lett 2006;6:96–100. doi:10.1021/nl052145f.

[10] Yu C, Shi L, Yao Z, Li D, Majumdar A. Thermal conductance and thermopower of an individual single-wall carbon nanotube. Nano Lett 2005;5:1842–6. doi:10.1021/nl051044e.

[11] Kim P, Shi L, Majumdar A, McEuen PL. Thermal Transport Measurements of Individual Multiwalled Nanotubes. Phys Rev Lett 2001;87:215502. doi:10.1103/PhysRevLett.87.215502.

[12] Hone J, Whitney M, Piskoti C, Zettl A. Thermal conductivity of single-walled carbon

nanotubes. Phys Rev B 1999;59:R2514–6. doi:10.1103/PhysRevB.59.R2514.

[13] Fujii M, Zhang X, Xie H, Ago H, Takahashi K, Ikuta T, et al. Measuring the Thermal Conductivity of a Single Carbon Nanotube. Phys Rev Lett 2005;95:65502.

[14] Pettes MT, Shi L. Thermal and structural characterizations of individual single-, double-, and multi-walled carbon nanotubes. Adv Funct Mater 2009;19:3918–25. doi:10.1002/adfm.200900932.

[15] Savas Berber and David Tománek Y-KK. Unusually High Thermal Conductivity of Carbon Nanotubes. Phys Rev Lett 2000;84:4613–6.

[16] Padgett CW, Brenner DW. Influence of chemisorption on the thermal conductivity of single-wall carbon nanotubes. Nano Lett 2004;4:1051–3. doi:10.1021/nl049645d.

[17] Che J, Cagin T, Goddard III WA. Thermal conductivity of carbon nanotubes. Nanotechnology 2000;11:65. doi:10.1088/0957-4484/11/2/305.

[18] Moreland JF. The disparate thermal conductivity of carbon nanotubes and diamond nanowires studied by atomistic simulation. Microscale Thermophys Eng 2004;8:61–9. doi:10.1080/10893950490272939.

[19] Bi K, Chen Y, Yang J, Wang Y, Chen M. Molecular dynamics simulation of thermal conductivity of single-wall carbon nanotubes. Phys Lett A 2006;350:150–3. doi:10.1016/j.physleta.2005.09.070.

[20] Cao A, Qu J. Size dependent thermal conductivity of single-walled carbon nanotubes. J Appl Phys 2012;112:13503. doi:10.1063/1.4730908.

[21] Zhou Q, Meng F, Liu Z, Shi S. The thermal conductivity of carbon nanotubes with defects and intramolecular junctions. J Nanomater 2013;2013. doi:10.1155/2013/842819.

[22] Han Z, Fina A. Thermal conductivity of carbon nanotubes and their polymer nanocomposites: A review. Prog Polym Sci 2011;36:914–44. doi:10.1016/j.progpolymsci.2010.11.004.

[23] Zhi C, Bando Y, Terao T, Tang C, Kuwahara H, Golberg D. Towards thermoconductive, electrically insulating polymeric composites with boron nitride nanotubes as fillers. Adv Funct Mater 2009;19:1857–62.

[24] Zhou B, Luo W, Yang J, Duan X, Wen Y, Zhou H, et al. Simulation of dispersion and alignment of carbon nanotubes in polymer flow using dissipative particle dynamics. Comput Mater Sci 2017;126:35–42. doi:10.1016/j.commatsci.2016.09.012.

[25] Kim YA, Kamio S, Tajiri T, Hayashi T, Song SM, Endo M, et al. Enhanced thermal conductivity of carbon fiber/phenolic resin composites by the introduction of carbon nanotubes. Appl Phys Lett 2007;90:1–4. doi:10.1063/1.2710778.

[26] Shenogin S, Bodapati A, Xue L, Ozisik R, Keblinski P. Effect of chemical functionalization on thermal transport of carbon nanotube composites. Appl Phys Lett 2004;85:2229–31.

[27] Salaway RN, Zhigilei L V. Molecular dynamics simulations of thermal conductivity of carbon nanotubes: Resolving the effects of computational parameters. Int J Heat Mass Transf 2014;70:954–64. doi:10.1016/j.ijheatmasstransfer.2013.11.065.

[28] Marconnet AM, Panzer MA, Goodson KE. Thermal conduction phenomena in carbon nanotubes and related nanostructured materials. Rev Mod Phys 2013;85:1295–326. doi:10.1103/RevModPhys.85.1295.

[29] Thomas JA, Iutzi RM, McGaughey AJH. Thermal conductivity and phonon transport in empty and water-filled carbon nanotubes. Phys Rev B - Condens Matter Mater Phys 2010;81:1–7. doi:10.1103/PhysRevB.81.045413.

[30] Mark JE. Physical properties of polymers handbook. 2007. doi:10.1524/zpch.1997.199.Part_1.128.

[31] Sengupta R, Chakraborty S, Bandyopadhyay S, Dasgupta S, Mukhopadhyay R, Auddy K, et al. A Short Review on Rubber / Clay Nanocomposites With Emphasis on Mechanical Properties. Engineering 2007;47:21–5. doi:10.1002/pen.

[32] Lukes JR, Zhong H. Thermal conductivity of individual single-wall carbon nanotubes. J Heat Transf 2007;129:705–16. doi:10.1115/1.2717242.

[33] Osman MA, Srivastava D. Temperature dependence of the thermal conductivity of single-wall carbon nanotubes. Nanotechnology 2001;12:21–4. doi:http://dx.doi.org/10.1088/0957-4484/12/1/305.

[34] Maruyama S, Engineering M, Taylor P. A molecular dynamics simulation of heat conduction in finite length SWNTs. Phys B Condens Matter 2002;323:41–50.

doi:10.1080/10893950390150467.

[35] Shiomi J, Maruyama S. Molecular dynamics of diffusive-ballistic heat conduction in single-walled carbon nanotubes. Jpn J Appl Phys 2008;47:2005–9. doi:10.1143/JJAP.47.2005.

[36] Walker AE. Influence of phonon modes on the thermal conductivity of single-wall, double-wall and functionalized carbon nanotubes. 2012.

[37] Hu G-J, Cao B-Y, Li Y-W. Thermal Conduction in a Single Polyethylene Chain Using Molecular Dynamics Simulations. Chinese Phys Lett 2014;31:86501. doi:10.1088/0256-307X/31/8/086501.

[38] Ye CM, Shentu BQ, Weng ZX. Thermal conductivity of high density polyethylene filled with graphite. J Appl Polym Sci 2006;101:3806–10. doi:10.1002/app.24044.

[39] Clancy TC, Gates TS. Modeling of interfacial modification effects on thermal conductivity of carbon nanotube composites 2006;47:5990–6. doi:10.1016/j.polymer.2006.05.062.

[40] Hu M, Yu D, Wei J. Thermal conductivity determination of small polymer samples by differential scanning calorimetry. Polym Test 2007;26:333–7.

[41] Zhong C, Yang Q, Wang W. Corrigendum to "Correlation and prediction of thermal conductivity of amorphous polymers":[Fluid Phase Equilibria 181 (2001) 195–202]. Fluid Phase Equilib 2001;192:209.

[42] Kline DE. Thermal conductivity studies of polymers. J Polym Sci 1961;50:441–50. doi:10.1002/pol.1961.1205015413.

[43] Zabihi Z, Araghi H. Effect of functional groups on thermal conductivity of graphene/paraffin nanocomposite. Phys Lett Sect A Gen At Solid State Phys 2016;380:3828–31. doi:10.1016/j.physleta.2016.09.028.

[44] Zhang Y-F, Zhao Y-H, Bai S-L, Yuan X. Numerical simulation of thermal conductivity of graphene filled polymer composites. Compos Part B Eng 2016;106:324–31. doi:10.1016/j.compositesb.2016.09.052.

[45] Hong W-T, Tai N-H. Investigations on the thermal conductivity of composites reinforced with carbon nanotubes. Diam Relat Mater 2008;17:1577–81.

[46] Cai D, Song M. Latex technology as a simple route to improve the thermal conductivity of a carbon nanotube/polymer composite. Carbon N Y 2008;46:2107–12.

[47] Gardea F, Lagoudas DC. Characterization of electrical and thermal properties of carbon nanotube/epoxy composites. Compos Part B Eng 2014;56:611–20. doi:10.1016/j.compositesb.2013.08.032.

[48] Yang K, Gu M, Guo Y, Pan X, Mu G. Effects of carbon nanotube functionalization on the mechanical and thermal properties of epoxy composites. Carbon N Y 2009;47:1723–37. doi:10.1016/j.carbon.2009.02.029.

[49] Zhou B, Luo W, Yang J, Duan X, Wen Y, Zhou H, et al. Thermal conductivity of aligned CNT/polymer composites using mesoscopic simulation. Compos Part A Appl Sci Manuf 2016;90:410–6. doi:10.1016/j.compositesa.2016.07.023.

[50] Wang Y, Iqbal Z, Malhotra S V. Functionalization of carbon nanotubes with amines and enzymes. Chem Phys Lett 2005;402:96–101.

[51] Ma PC, Tang BZ, Kim J-K. Effect of CNT decoration with silver nanoparticles on electrical conductivity of CNT-polymer composites. Carbon N Y 2008;46:1497–505.

[52] Liu P. Modifications of carbon nanotubes with polymers. Eur Polym J 2005;41:2693–703.

[53] Geng Y, Liu MY, Li J, Shi XM, Kim JK. Effects of surfactant treatment on mechanical and electrical properties of CNT/epoxy nanocomposites. Compos Part A Appl Sci Manuf 2008;39:1876–83.

[54] Gulotty R, Castellino M, Jagdale P, Tagliaferro A, Balandin AA. Effects of functionalization on thermal properties of single-wall and multi-wall carbon nanotube–polymer nanocomposites. ACS Nano 2013;7:5114–21. doi:10.1021/nn400726g.

[55] Bhattacharya M. Polymer nanocomposites-A comparison between carbon nanotubes, graphene, and clay as nanofillers. Materials (Basel) 2016;9:1–35. doi:10.3390/ma9040262.

[56] Desai TG, Lawson JW, Keblinski P. Modeling initial stage of phenolic pyrolysis: Graphitic precursor formation and interfacial effects. Polymer (Guildf) 2011;52:577–85. doi:10.1016/j.polymer.2010.11.018.

[57] Hwang MJ, Stockfisch TP, Hagler AT. Derivation of class II force fields. 2. Derivation and characterization of a class II force field, CFF93, for the alkyl functional group and alkane molecules. J Am Chem Soc 1994;116:2515–25.

[58] Tersoff J. Modeling solid-state chemistry: Interatomic potentials for multicomponent systems. Phys Rev B 1989;39:5566–8. doi:10.1103/PhysRevB.39.5566.

[59] Stuart SJ, Tutein AB, Harrison JA. A reactive potential for hydrocarbons with intermolecular interactions. J Chem Phys 2000;112:6472–86. doi:10.1063/1.481208.

[60] Brenner DW, Shenderova OA, Harrison JA, Stuart SJ, Ni B, Sinnott SB. A second-generation reactive empirical bond order (REBO) potential energy expression for hydrocarbons. J Phys Condens Matter 2002;14:783–802. doi:10.1088/0953-8984/14/4/312.

[61] Lindsay L, Broido DA. Optimized Tersoff and Brenner empirical potential parameters for lattice dynamics and phonon thermal transport in carbon nanotubes and graphene. Phys Rev B - Condens Matter Mater Phys 2010;81:1–6. doi:10.1103/PhysRevB.81.205441.

[62] Lee JG. Computational materials science: an introduction. 2012.

[63] Griebel M, Knapek S, Zumbusch G. Numerical Simulation in Molecular Dynamics. 2007.

[64] Tersoff J. New empirical approach for the structure and energy of covalent systems. Phys Rev B 1988;37:6991–7000. doi:10.1103/PhysRevB.37.6991.

[65] Tersoff J. Empirical interatomic potential for carbon, with applications to amorphous carbon. Phys Rev Lett 1988;61:2879–82. doi:10.1103/PhysRevLett.61.2879.

[66] Brenner D. Empirical potential for hydrocarbons for use in simulating the chemical vapor deposition of diamond films. Phys Rev B 1990;42:9458–71. doi:10.1103/PhysRevB.42.9458.

[67] Sun H. COMPASS: An ab Initio Force-Field Optimized for Condensed-Phase Applications s Overview with Details on Alkane and Benzene Compounds 1998;5647:7338–64.

[68] Zhong H, Lukes JR. Thermal conductivity of single-wall carbon nanotubes. Proc.

ASME Int. Mech. Eng. Congr. Expo., 2004.

[69] Accelrys Software Inc. Discovery Studio Modeling Environment, Release 8.0. Accelrys Software Inc., San Diego 2017.

[70] S. Plimpton. Fast Parallel Algorithms for Short-Range Molecular Dynamics. J Comp Phys 1995;117:1–19.

[71] Müller-Plathe F. A simple nonequilibrium molecular dynamics method for calculating the thermal conductivity. J Chem Phys 1997;106:6082. doi:10.1063/1.473271.

APPENDIX A : MD script for thermal conductivity of SWCNT

```
#___Simulation of thermal conductivity for a single-walled carbon nanotube___#
clear
log "C:\ACmp\Project\ten ten swcnt\length\output\out1000.txt"
#___Initialization__#
echo screen
units metal
dimension 3
atom_style atomic
boundary p p p
#___Atom definition___ #
read_data "C:\ACmp\Project\ten ten swcnt\length\cnt data file\1000.txt"
region cold block INF INF INF INF 0 1000 units box
region tube block INF INF INF INF 1000 9000 units box
region hot block INF INF INF INF 9000 10000 units box
 #___Settings and Simulation___#
pair_style tersoff
pair_coeff * * BNC.tersoff C
group cold region cold
group hot region hot
group tube region tube
group nowalls union cold tube hot
#___1st EQUILIBRATION___#
neighbor 2.0 bin
neigh_modify every 3 delay 3
velocity nowalls create 300.0 42020
fix 1 nowalls nvt temp 300 300 .1
thermo 1000
dump frtdump1 nowalls custom 5000 "C:\ACmp\Project\ten ten
swcnt\length\dump1\nvt1000.lammpstrj" id type x y z ix iy iz
```

run 100000

velocity nowalls scale 300

unfix 1

#___ 1st Heat Flux___#

compute ke nowalls ke/atom

variable temp atom c_ke/1.5/8.617343e-5

fix 1 nowalls nve

compute layers nowalls chunk/atom bin/1d z lower .02 units reduced

fix 2 nowalls ave/chunk 10 100 1000 layers v_temp file "C:\ACmp\Project\ten ten swcnt\length\profile\1000temp.profile"

fix 3 nowalls thermal/conductivity 10 z 20

variable tdiff equal f_2[26][3]-f_2[1][3]

thermo_style custom step temp epair etotal f_3 v_tdiff

thermo 1000

#dump frtdump2 nowalls custom 5000 "C:\ACmp\Project\ten ten swcnt\length\dump1\1nve1000.lammpstrj" id type x y z ix iy iz

run 1000000

log "C:\ACmp\Project\ten ten swcnt\length\output\cal1000.txt"

#___thermal conductivity calculation___#

fix 3 nowalls thermal/conductivity 10 z 20

fix ave nowalls ave/time 1 1 1000 v_tdiff ave running

thermo_style custom step temp epair etotal f_3 v_tdiff f_ave

thermo 1000

#dump frtdump3 nowalls custom 5000 "C:\ACmp\Project\ten ten swcnt\length\dump1\2nve1000.lammpstrj" id type x y z ix iy iz

run 1000000

Data file – 1000.txt

162880 atoms

1 atom types

-50 50 xlo xhi

-50 50 ylo yhi

-0.61377 10000.4 zlo zhi

Masses

1 12

Atoms

1 1 6.77974 0 0

2 1 6.63159 1.40959 0

3 1 6.44792 2.09506 1.22802

4 1 5.87143 3.38987 1.22802

5 1 5.48493 3.98503 0

…….

162877 1 5.48493 -3.98503 9998.57

162878 1 6.1936 -2.75757 9998.57

162879 1 6.44792 -2.09506 9999.8

162880 1 6.7426 -0.708676 9999.8

APPENDIX B : MD Script for thermal conductivity of Polyethylene polymer

```
#___Simulation of thermal conductivity for polyethylene___#
log "C:\Users\Administrator\Desktop\c5pe200\log\10.txt"
# ___Initialization___#
  Clear
  echo screen
  units real
  boundary p p p
  atom_style full
   bond_style class2
   angle_style class2
   dihedral_style class2
   improper_style class2
   pair_style lj/class2 10.0
   pair_modify mix geometric
#___Atom definition___ #
read_restart "C:\Users\Administrator\Desktop\c5pe200\min\4.7.restart"
# 4.7.restart file contains the required state of the simlulation that achieved during
equilibration.
#___Settings and Simulation___#
group polymer type 1 2 3
velocity polymer create 300.0 12456 dist gaussian units box
neighbor 2.0 bin
neigh_modify delay 0 every 1 check yes one 4000 page 250000
reset_timestep 0
timestep 0.1
thermo 1000
#___1st Equilibrium___#
fix 1 polymer nvt temp 300 300 100
```

```
thermo 1000

run 2000000

velocity polymer scale 300

unfix 1

#___1st Heat Flux___#

compute ke polymer ke/atom

variable temp atom c_ke/1.5/8.617343e-5/23.0607812

fix 1 polymer nve

compute layers polymer chunk/atom bin/1d z lower .02 units reduced

fix 2 polymer ave/chunk 10 100 1000 layers v_temp file
"C:\Users\Administrator\Desktop\c5pe200\profile\c5pe200temp.profile"

fix 3 polymer thermal/conductivity 100 z 20

variable tdiff equal f_2[26][3]-f_2[1][3]

thermo_style custom step temp epair etotal f_3 v_tdiff density lx ly lz

thermo 1000

dump frtdump2 polymer custom 5000
"C:\Users\Administrator\Desktop\c5pe200\dump1\1nvec5pe200.lammpstrj" id mol type x y z
ix iy iz

run 5000000

log "C:\Users\Administrator\Desktop\c5pe200\output\calc5pe200.txt"

#___thermal conductivity calculation____#

fix 3 polymer thermal/conductivity 100 z 20

fix ave polymer ave/time 1 1 1000 v_tdiff ave running

thermo_style custom step temp epair etotal f_3 v_tdiff f_ave density lx ly lz

thermo 1000

dump frtdump3 polymer custom 5000
"C:\Users\Administrator\Desktop\c5pe200\dump1\2nvec5pe200.lammpstrj" id mol type x y z
ix iy iz

run 5000000
```

APPENDIX C : MD Script for thermal conductivity of functionalized SWCNT/polyethylene nanocomposites

```
log "C:\Users\Administrator\Desktop\c5pe200f5\log\10.txt"
#___Initialization__#
 Clear
    echo screen
    units real
    boundary p p p
    atom_style full
    bond_style class2
    angle_style class2
    dihedral_style class2
    improper_style class2
    pair_style lj/class2 10.0
    pair_modify mix geometric
#___Atom definition___ #
read_restart "C:\Users\Administrator\Desktop\c5pe200f5\min\4.7.restart"
# 4.7.restart file contains the required state of the simlulation that achieved during
equilibration
#___Settings and Simulation___#
# group CNT type 1 2
# group polymer type  3 4 5 6 7 8 9
velocity all create 300.0 12456 dist gaussian units box
 neighbor 2.0 bin
neigh_modify delay 0 every 1 check yes one 4000 page 250000
reset_timestep 0
timestep 0.1
thermo 1000
#___1st EQUILIBRATION___#
fix 1 all nvt temp 300 300 100
thermo 1000
```

```
run 2000000

velocity all scale 300

unfix 1


#___1st Heat Flux___#

compute ke all ke/atom

variable temp atom c_ke/1.5/8.617343e-5/23.0607812

fix 1 all nve

compute layers all chunk/atom bin/1d z lower .02 units reduced

fix 2 all ave/chunk 10 100 1000 layers v_temp file
"C:\Users\Administrator\Desktop\55cnt200pef5\profile\55cnt200pef5temp.profile"

fix 3 all thermal/conductivity 100 z 20

variable tdiff equal f_2[26][3]-f_2[1][3]

thermo_style custom step temp epair etotal f_3 v_tdiff density lx ly lz

thermo 1000

dump frtdump2 all custom 5000
"C:\Users\Administrator\Desktop\55cnt200pef5\dump1\1nve55cnt200pef5.lammpstrj" id mol
type x y z ix iy iz

run 5000000

log "C:\Users\Administrator\Desktop\55cnt200pef5\output\cal55cnt200pef5.txt"

#___thermal conductivity calculation____#

fix 3 all thermal/conductivity 100 z 20

fix ave all ave/time 1 1 1000 v_tdiff ave running

thermo_style    custom step temp epair etotal f_3 v_tdiff f_ave density lx ly lz

thermo 1000

dump frtdump3 all custom 5000
"C:\Users\Administrator\Desktop\55cnt200pef5\dump1\2nve55cnt200pef5.lammpstrj" id mol
type x y z ix iy iz

run 5000000
```

Effect of functionalization on the thermal conductivity of CNT/polymer nanocomposites using reverse non-equilibrium molecular dynamics simulations

ORIGINALITY REPORT

%10	%3	%9	%
SIMILARITY INDEX	INTERNET SOURCES	PUBLICATIONS	STUDENT PAPERS

PRIMARY SOURCES

1	Khan, Asir, Ishtiaque Navid, Maliha Noshin, H. Uddin, Fahim Hossain, and Samia Subrina. "Equilibrium Molecular Dynamics (MD) Simulation Study of Thermal Conductivity of Graphene Nanoribbon: A Comparative Study on MD Potentials", Electronics, 2015. Publication	%1
2	nanoelectronics.ch Internet Source	%1
3	Zhong, Hongliang, and Jennifer R. Lukes. "Thermal Conductivity of Single-Wall Carbon Nanotubes", Electronic and Photonic Packaging Electrical Systems Design and Photonics and Nanotechnology, 2004. Publication	%1
4	www.ndl.ee.ucr.edu Internet Source	%1
5	Pan Rui-Qin. "Length Dependence of Thermal	